AD-A111 113 UNITED TECHNOLOGIES RESEARCH CENTER EAST HARTFORD CT F/G 11/6
DEFORMATION STUDIES IN WORKABLE SUPERALLOYS.(U)
NOV 81 A F GIAMEI F49620-80-C-0004
UNCLASSIFIED R81-213713-1 AFOSR-TR-82-0026 NL

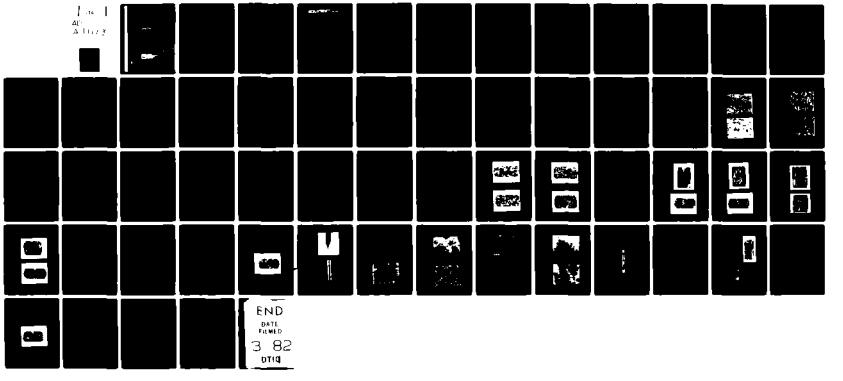

END
DATE FILMED
3 82
DTIC

AFOSR-TR- 82 -0026

R81-213713-1

LEVEL II

DEFORMATION STUDIES IN WORKABLE SUPERALLOYS

Prepared by
Anthony F. Giamei

Final ANNUAL REPORT

Contract F49620-80-C-0004

for

Air Force Office of Scientific Research
Washington, DC 20332

November 30, 1981

AD A111113

DTIC FILE COPY

DTIC
ELECTE
FEB 19 1982
S D
A

UNITED TECHNOLOGIES RESEARCH CENTER

Approved for public release;
distribution unlimited.
81-12-8-1

82 02 18 026

Unclassified

SECURITY CLASSIFICATION OF THIS PAGE (When Data Entered)

REPORT DOCUMENTATION PAGE		READ INSTRUCTIONS BEFORE COMPLETING FORM
1. REPORT NUMBER AFOSR-TR- 82-0026	2. GOVT ACCESSION NO. AD-A111 113	3. RECIPIENT'S CATALOG NUMBER
4. TITLE (and Subtitle) Deformation Studies in Workable Superalloys		5. TYPE OF REPORT & PERIOD COVERED Final 10/1/79 - 9/30/81
		6. PERFORMING ORG. REPORT NUMBER
7. AUTHOR(s) Anthony F. Giamei		8. CONTRACT OR GRANT NUMBER(s) F49620-80-C-0004
9. PERFORMING ORGANIZATION NAME AND ADDRESS Pratt & Whitney Aircraft/UTRC United Technologies Corporation East Hartford, Connecticut 06108		10. PROGRAM ELEMENT, PROJECT, TASK AREA & WORK UNIT NUMBERS 61102F 2306-A1
11. CONTROLLING OFFICE NAME AND ADDRESS Air Force Office of Scientific Research Bolling Air Force Base, D. C. 20332		12. REPORT DATE November 30, 1981
		13. NUMBER OF PAGES 55
14. MONITORING AGENCY NAME & ADDRESS (if different from Controlling Office)		15. SECURITY CLASS. (of this report) Unclassified
		15a. DECLASSIFICATION/DOWNGRADING SCHEDULE

16. DISTRIBUTION STATEMENT (of this Report)

Approved for public release; distribution unlimited.

17. DISTRIBUTION STATEMENT (of the abstract entered in Block 20, if different from Report)

18. SUPPLEMENTARY NOTES

19. KEY WORDS (Continue on reverse side if necessary and identify by block number)

Workability	Strain Rate Sensitivity
Plastic Strain	High Cooling Rate
Isothermal Forming	Recrystallization

20. ABSTRACT (Continue on reverse side if necessary and identify by block number)

The second and final year of a workability study of nickel-base superalloys is now complete. The objective was to study the high strain plastic flow behavior of high strength superalloys in the form of single crystals, rapidly solidified ingots and consolidated powder particles. The single crystal alloy studied was PWA 1444 (similar to Mar-M200) which had previously been well characterized at low strains. The flow characteristics of this alloy have now been documented out to 15% strain as a function of crystal orientation. The low to intermediate

DD FORM 1 JAN 73 1473 EDITION OF 1 NOV 65 IS OBSOLETE

SECURITY CLASSIFICATION OF THIS PAGE (When Data Entered)

Block 20 (continued)

temperature flow stress has been measured after forming. Remarkable work hardening has been obtained at low strains for high modulus crystals worked below the solvus temperature. Rapidly solidified and cooled ingots were made by arc melting or electron beam skull melting or induction melting and then "drip melting" into a cold copper mold. The compositions and heat treatment were tailored to promote workability. Some of these buttons were heavily deformed in uniaxial compression under isothermal conditions below the gamma prime solvus temperature, and several were deformed in the single phase gamma region. High strains were achieved under conditions of constant displacement rate, true strain rate or energy input rate. These materials have been deformed to 90% reduction in height (true strain $\simeq -2.3$) above the solvus without cracking. A range of forming temperatures has been investigated. The strain dependence of grain size has been investigated at 15% strain intervals during dynamic recrystallization. A fine grained structure has been created by cooling through the gamma prime solvus temperature during the forming operation. The powder base line material, PWA 1056 (IN-100), was shown to be superplastic by strain rate sensitivity measurement using stress change experiments centered around a strain rate of 0.2% S^{-1} (10% min^{-1}). The strain dependence of the strain rate sensitivity has now been defined as well as the grain size dependence. The strain rate was varied from 2×10^{-3}% S^{-1} to 1.5×10^{1}% S^{-1}.

UNITED TECHNOLOGIES RESEARCH CENTER

UNITED TECHNOLOGIES

East Hartford, Connecticut 06108

R81-213713-1

Deformation Studies in Workable Superalloys

~~Second Annual~~ Report
Contract F49620-80-C-0004

REPORTED BY Anthony J. Giamei
A. F. Giamei

AIR FORCE OFFICE OF SCIENTIFIC RESEARCH (AFSC)
NOTICE OF [illegible]
This tech[illegible] reviewed and is
approved [illegible] 190-12.
Distribut[illegible].
MATTHEW J. KE[illegible]
Chief, Technical [illegible] Division

APPROVED BY
F. L. VerSnyder, Ass't. Dir.
of Research for Materials Tech.

DATE 11/30/81

NO. OF PAGES 53

COPY NO. _____

R81-213713-1

Deformation Studies in Workable Superalloys

TABLE OF CONTENTS

1.0 ABSTRACTS 1

1.1 Program Overview 1
1.2 Technical Progress 2

2.0 INTRODUCTION 3

3.0 PROGRESS 8

3.1 Consolidated Powder 9
3.2 Rapidly Solidified Structures 11
3.3 Single Crystals 14
3.4 Acknowledgement 18

FIGURES 1 - 31 19

4.0 REFERENCES 51

5.0 PUBLICATIONS AND PRESENTATIONS FROM AFOSR SPONSORED WORK 53

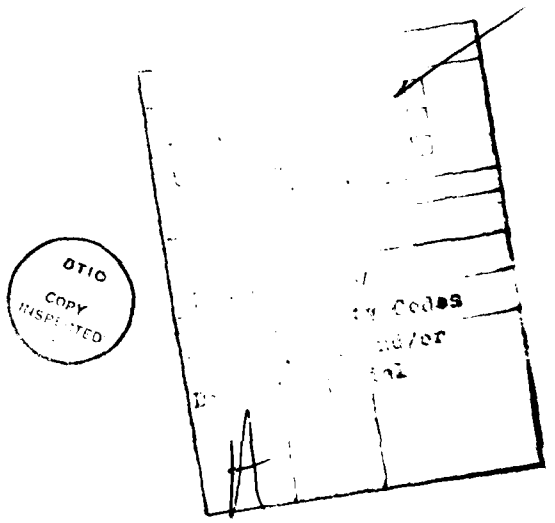

R81-213713-1

Deformation Studies in Workable Superalloys

1.0 ABSTRACTS

1.1 Program Overview

The third and final year of a program has been proposed (P81-250, 8/11/81) to systematically study, from a fundamental point of view, nickel base superalloy high temperature plastic flow behavior under carefully controlled experimental conditions in a variety of alloy chemistries and microstructures. This work would relate to high performance applications for superalloy gas turbine disks made from materials without significant residual chemical macrosegregation. (These can be prepared by relatively high cooling rate techniques.) The object of this research is to define the physical and structural aspects of the large strain plastic flow behavior of homogeneous nickel alloys under precisely defined conditions of deformation temperature and energy input rate. The approach would be to prepare rapidly cooled alloys with various amounts of gamma prime formers present, minimize the presence of significant macrosegregation by solidification process selection and eliminate most or all of any residual microsegregation by homogenization heat treatment, and form to large strains (such as an engineering strain of -60 percent or a true strain of -0.92) under computer controlled conditions such as constant temperature and true plastic strain rate. This would be carried out above and below the gamma prime solvus temperature with an on-line computer monitoring actual displacement, displacement rate, engineering strain rate, true strain rate, energy input rate, load, engineering stress and true flow stress to anticipate the onset of dynamic recrystallization, which will subsequently be checked microstructurally. The isothermal strain rate sensitivity will be measured to anticipate superplastic behavior, post formed deformation behavior will be documented and materials will be examined for the onset of grain boundary cracking as it may relate to various chemistry and microstructural considerations, workability theory (such as compatibility requirements for matrix and grain boundary strength, or any potentially new deformation mechanisms based on observed dislocation configurations before and after plastic flow. It is expected that a third year will complete this effort. This work would be directed toward the characterization of microstructures and plastic flow properties in materials made by rapid cooling from the liquid state and comparisons with conventional superalloy disk materials such as forged castings or consolidated powder. A considerable effort will be made to study the dynamics of the recrystallization process. An improved understanding

of static and dynamic recrystallization in high strength superalloys will lead to the finest possible grain size after forming. This will, in turn, lead to improvements in yield strength, ultimate strength and fatigue resistance.

1.2 Technical Progress

The second year of a proposed three year workability study of nickel-base superalloys is now complete. The objective was to study the high strain plastic flow behavior of high strength superalloys in the form of single crystals, rapidly solidified ingots and consolidated powder particles. The single crystal alloy studied was PWA 1444 (similar to Mar-M200) which had previously been well characterized at low strains. The flow characteristics of this alloy have now been documented out tc 15% strain as a function of crystal orientation. The low to intermediate temperature flow stress has been measured after forming. Remarkable work hardening has been obtained at low strains for high modulus crystals worked below the solvus temperature. Rapidly solidified and cooled ingots were made by arc melting or electron beam skull melting or induction melting and then "drip melting" into a cold copper mold. The compositions and heat treatment were tailored to promote workability. Some of these buttons were heavily deformed in uniaxial compression under isothermal conditions below the gamma prime solvus temperature, and several were deformed in the single phase gamma region. High strains were achieved under conditions of constant displacement rate, true strain rate or energy input rate. These materials have been deformed to 90% reduction in height (true strain ≈ -2.3) above the solvus without cracking. A range of forming temperatures has been investigated. The strain dependence of grain size has been investigated at 15% strain intervals during dynamic recrystallization. A fine grained structure has been created by cooling through the gamma prime solvus temperature during the forming operation. The powder base line material, PWA 1056 (IN-100), was shown to be superplastic by strain rate sensitivity measurement using stress change experiments centered around a strain rate of 0.2% S^{-1} (10% min^{-1}). The strain dependence of the strain rate sensitivity has now been defined as well as the grain size dependence. The strain rate was varied from 2×10^{-3} % S^{-1} to 1.5×10^{1} % S^{-1}.

2.0 INTRODUCTION

Improved performance in modern gas turbine engines has traditionally been achieved by greater turbine inlet temperature, or greater rotor speed, or both. These parameters increase the efficiency or thrust but place greater demands on the turbine blades, and therefore turbine disks. Substantial improvements in turbine blade performance are promised by directional solidification (DS) (Ref. 1) including single crystal components (SC) (Ref. 2), directional recrystallization (DR), fiber reinforced superalloys (FRS) or eutectics (Ref. 3). The recent disk advances have centered around lowering density, cost and/or raw material utilization. With new requirements of higher disk alloy strengths, or longer lives, it will be necessary to gain a better understanding of nickel-base superalloy disk forming operations.

A brief review of superalloy disk working regimes as they relate to alloy composition and microstructure is in order. Alloys with low volume fraction of strengthening phase (Ni_3Ti, Ni_3Nb or Ni_3Al) are referred to as lean superalloys, e.g. Waspaloy, and are normally cast as ingots, preheated to above the solvus temperature, and worked with relative ease. On the other hand, intermediate strength (and gamma prime volume fraction) superalloys, such as Astroloy, are again cast as ingots, but are worked just below the gamma prime solvus temperature with great care, particularly at low strain, to avoid grain boundary cracking (Ref. 4). Warm die forging is generally used with intermediate annealing.

The high strength superalloys represent a real challenge. These alloys can, on occasion, be cast as ingots, heat treated and worked successfully. However, these results are not reproducible from billet to billet, and alloys such as cast IN-100 or MAR-M200 are generally considered to be unworkable. It is known that these results are due, at least in part, to the influence of macrosegregation on the microstructure (Ref. 5). Substantial variations in the amount of aluminum and/or titanium lead to local differences in the amount of eutectic gamma prime, and therefore the local response to heat treatment. Residual microsegregation can lead to incipient melting at anomalously low temperatures.

It is unfortunate that the higher solute ("hardener") content superalloys are more prone to macrosegregation and seem to have a lower level of intrinsic grain boundary strength. This dilemma, as well as the promise of substantial improvements in the "fly/buy" ratio, fostered the advent of the powder metallurgy approach to making superalloy disks (Ref. 6). This method ensures the lack of substantial macrosegregation by the nature of the powder making process. The residual short wavelength microsegregation patterns are virtually eliminated

by consolidation steps such as hot isostatic pressing (HIP) or Gatorizing® or extrusion. The fine particle size (10-100μm) of the powder particles leads to superplastic flow in closed die isothermal forming (Ref. 7). The high ductility as well as the low flow stress are useful in making large complex shapes.

Further advances in powder metallurgy will require: tailoring the alloy to the processing methods to avoid both carbide precipitation at prior particle boundaries and incipient melting; minimization of inclusion content and size, leading to an extension of cyclic fatigue life; local grain size coarsening to enhance creep life; local thermo-mechanical strengthening (Ref. 8) to boost yield and/or ultimate tensile strength; and possibly local chemistry or particle size variations to achieve the desired level of creep resistance at the rim and fatigue resistance at the bore. We need more fundamental knowledge about these materials if these challenges are going to be met.

There may also be a path available to obtain substantial workability in cast high strength superalloys by combining the control of local composition and forming conditions. We have done some interesting experiments on model superalloys, and some of the supposedly unworkable alloys. First, fine dendritic structures were obtained. This can be done over a short distance by using a water cooled copper chill surface, e.g., in an arc melted button, a drop casting or the lower end of a DS casting (Ref. 9). On a larger scale, drip melted ingots can be made in cold or cooled molds by clean melting techniques such as electric arc or electron beam. These techniques have the added advantage of avoiding ceramic contamination, and possibly reducing or volatilizing pre-existing inclusions. The ceramic contaminants tend to float and can be substantially reduced by skimming methods.

The primary and secondary dendrite arm spacings are related to cooling rate (Ref. 10) as follows:

$$S_1 \sim \left(\frac{\Delta T}{G \cdot R}\right)^m = \left(\frac{\Delta T}{\dot{T}}\right)^m, \quad m \cong 0.25 \tag{1}$$

$$S_2 \sim \left(\frac{\Delta T}{G \cdot R}\right)^n = \left(\frac{\Delta T}{\dot{T}}\right)^n, \quad 0.3 < n \leq 0.5 \tag{2}$$

where ΔT is the melting range of the alloy of interest, G is the thermal gradient perpendicular to the liquidus surface and R is the growth rate, the rate-gradient product is equal to the cooling rate, $\dot{T}$, as established below:

$$G \cdot R = \frac{\Delta T}{\Delta Z} \cdot \frac{\Delta Z}{\Delta t} = \frac{\Delta T}{\Delta t} = \dot{T} \tag{3}$$

and G is related to the melting range and the mushy zone height, ΔZ, as follows:

$$G = \frac{\Delta T}{\Delta Z} = \frac{T_L - T_S}{Z_L - Z_S} \tag{4}$$

where L and S represent the alloy liquidus and solidus temperatures, respectively.

The fine dendrite structures can now be wholly or partially eliminated according to the relationship (Refs. 11,12):

$$t_h \sim S_1^2 \tag{5}$$

where t_h is the time required to obtain a given state of homogenization. Combining Eq. 1 and 5, we have:

$$t_h \sim (\dot{T})^{-\frac{1}{2}} \tag{6}$$

Based on a limited number of observations with two Ni-Al-Ta alloys, the proportionality constant is approximately 10^5 when t is in seconds and $\dot{T}$ is in °C/second. The implications of Eq. 6 for several alloy processing schemes are given in Table I.

"Normal" DS might be typical of a microstructure found 3-5 cm from the chill plate. Actual DS structures range from this base line by about a factor of ten in cooling rate to either side if liquid metal cooling (LMC) is included (Ref. 13). The "thin zone" DS structure is simply an idealization of a drip melted ingot where cooling of each new layer is by conduction to the cold ingot below as well as radiation to the environs. Layerglazing is a process where an extremely thin melt layer is formed by surface melting of a cold ingot by using a laser pulse or scan. RSR is a rapid solidification rate powder making process. Low pressure plasma spray (LPPS) is a means of generating 98-99% dense material with little risk of oxidation of entrapment of gas. Many of the cooling rates are calculated rather than measured, but the potential advantages of rapid cooling (Ref. 14) are obvious.

Table I

Approximate Theoretical Times to 80% Homogenization at ~1315°C for Tantalum in Nickel with Various Processes. (Assumes Only Microsegregation)

Process	$\dot{T}$ (°C/s)	$(\dot{T})^{\frac{1}{2}}$	$(\dot{T})^{-\frac{1}{2}}$	t_h (sec)	t_h (hr)
Large Ingot	10^{-2}	10^{-1}	10	10^6	278
Normal DS	1	1	1	10^5	28
Thin Zone DS	10^2	10	0.1	10^4	2.8
Drop Casting	10^4	10^2	10^{-2}	10^3	0.28
Layerglaze, RSR or LPPS	10^6	10^3	10^{-3}	10^2	0.028

The second key feature is the use of an intermediate strain rate isothermal forming process. This had been carried out in a model ternary alloys (Ni-Al-Ta) selected to simulate high γ' volume fraction superalloys. These alloys were strained to 60% reduction in height in either a continuous or interrupted mode at nearly constant true strain rate above the solvus temperature. The significant aspect of the aforementioned deformation work was thought to be the excellent homogenizability afforded by high cooling rates during solidification combined with the high solidus temperatures of the model alloy (~1400°C). The flow stress curve below the solvus temperature in these alloys shows a high initial flow stress plus strain hardening, whereas the flow stress initiates and stays at a low level at temperatures above the solvus due to dynamic recrystallization.

MAR-M200 and cast IN-100 have also been formed up to 60% engineering strain by isothermal forming at controlled true strain rate above the solvus temperature. Fine dendritic structures (capable of near homogenization in short times) were available in DS castings from 2-5 cm above the chill. MAR-M200 can be annealed at 1260°C without melting if a gradual approach to the high temperature is used. The following conditions can be used for homogenization: 1204°C/2 hr + 1232°C/2 hr + 1260°C/20 hr. This treatment almost completely eliminated dendritic segregation in PWA 664 at the 3 cm level (up from the chill). This material could be deformed in much the same manner as the modified IN-100 alloy, using a function generator and a hydraulic test frame.

Consistent with earlier observations, it was not possible to reproducibly work cast IN-100, or cast + extruded, or cast ingots of the powder version. There are cases where high volume fraction gamma prime alloys could be consistently formed, namely Ni-Al-Ta model superalloys. Additionally, the intermediate volume fraction alloy Udimet 700 can also be readily worked above the solvus temperature to very high strains without cracking. These alloys had a gap between solidus and solvus, which is not the case for IN-100, nor most of its many modifications. Therefore, the most effective modification of the IN-100 alloy was to slightly decrease the solvus temperature by altering the gamma prime forming elements.

Thus IN-100 can sometimes be worked by an isothermal forming approach starting with extruded ingots or rapidly cooled arc melted buttons. It would appear that modified IN-100 can be prepared in large sizes without macrosegregation and with the high cooling rates essential for the elimination of most, if not all, microsegregation by electron beam melting of a stick, or ingot, and dripping into a chill mold. An 8 cm diameter ingot has been prepared as a preliminary demonstration that such a material can be homogenized and formed. There is still more to be done, but such an approach seems very promising. LPPS will also be examined as a high cooling rate alternative which may be easier to control on a fine scale. Both the drip melted material and its alternatives (Layerglaze or LPPS) would probably require a HIP or extrusion cycle.

3.0 PROGRESS

Superalloys have excellent high temperature properties due to the presence of the coherent ordered precipitate, gamma prime (γ'). From a workability point of view, we can separate such alloys into three main categories: low, intermediate and high strength (or hardener content or volume fraction γ') superalloys. The low strength alloys, e.g., Waspaloy, are easily hot worked above the γ' solvus temperature; the intermediate strength alloys, e.g., Astroloy, are worked (with some difficulty) below the γ' solvus; the high strength alloys such as IN-100 are generally considered unworkable in any condition other than as a consolidated (superplastic) powder metallurgy product (Refs. 15,16).

Previous fundamental alloy studies programs carried out at Pratt & Whitney Aircraft have suggested that good workability in alloys such as IN-100 and even MAR-M200 could be obtained even with a relatively coarse cast grain size and microstructure. The following seemed to be important desirable factors for workability during high strain uniaxial compression testing:

1) near elimination of residual microsegregation
2) isothermal conditions
3) approximately constant true strain rate, and
4) <u>small</u> amounts of carbide or eutectic γ' phases to act as nucleation sites for recrystallization.

Item (1) dictates a high cooling rate if the homogenization is to be done in a reasonable time. Item (2) is easily achieved in the kind of equipment available today. Item (3) was only crudely carried out in previous studies by combining several short strokes or by periodically adjusting the displacement rate based on prior calculations. This program has improved on these relatively crude techniques with the utilization of a process control computer. One objective was to control the rate of energy input rather than the load or displacement rate. Item (4) is neither fully established nor understood in any great detail.

The general approach in the first year was to establish a powder metallurgy base line for the F100 first-stage turbine disk bill of material in terms of such variables as flow stress and strain rate sensitivity parameter. The flow characteristics were determined at several temperatures near, but below, the γ' solvus. Next, the high strain behavior was compared for rapidly cooled bulk alloys in between U-700 and IN-100 at temperatures above the solvus. Obviously, a gap between solvus and solidus is desirable for the maximum degree of flexibility in the control of microstructure. Another type of rapidly cooled

bulk alloy (starting with arc or electron beam melted buttons) under study was an equiaxed version of the single crystal alloy 444 (PWA 1444) which was selected because it represents a fully characterized alloy based on Pratt & Whitney Aircraft and Air Force Office of Scientific Research sponsored work and because it allows the opportunity to deduce the effect of grain boundaries or to study the anisotropy effects or to simplify the analytical problem by the elimination of grain boundaries.

During the second year a rather complete characterization of the log stress-log strain rate relationship was completed for the powder base line. Nearly four decades of strain rate were covered. The strain rate sensitivity can now be accurately obtained as a function of both strain and strain rate. Some of the powder material was intentionally grain size coarsened to assess the importance of grain size on superplasticity. The rapidly cooled cast structures were made in larger sizes so that post formed properties could be measured. It was decided to concentrate on a modification of IN-100 which proved to be quite workable. Finally, single crystals of PWA 1444 were prepared in <001>, <110> and <111> orientations and work hardening studies were carried out to 10% strain at two temperatures below the solvus.

3.1 Consolidated Powder

Normally, the PWA 1056 powder billet was worked at 1080°C, which is below the γ' solvus temperature. The grain size is relatively stable at that temperature for 1-2 hr. However, at temperatures in the range 1150-1200°C, the grain size coarsens rapidly. In the first year of this program, the strain rate sensitivity, m, was determined to be 0.70 at 1070°C in the range 0.2 to 2% S^{-1}. The parameter m, or strain rate sensitivity is defined as follows:

$$\sigma = A \dot{\varepsilon}^{m} \tag{7}$$

$$\ln \sigma = \ln A + m \ln \dot{\varepsilon} \tag{8}$$

$$m = \frac{d \ln \sigma}{d \ln \dot{\varepsilon}} \tag{9}$$

The strain rate sensitivity can be determined from a stress change, or directly from a plot of $\ln \sigma$ vs. $\ln \dot{\varepsilon}$. Figure 1 shows such a plot for three grain size conditions in PWA 1056. The data were collected at 1080°C. The as-extruded material shows m = 0.68 in the strain rate range of 0.25 to 1.5% S^{-1}, while m drops to 0.36 (still superplastic) for powder material slightly coarsened by

1150°C/4 hr/AC treatment. The parameter m falls to 0.16 (out of the range of superplastic behavior) when the treatment is 1200°C/4 hr/AC. These observations were further substantiated by some cracking in the forming of 1200°C annealed material. Note the apparent linearity of the data over the measured strain rate range. These data are considered to be quite valuable in that the coarsening effect is quite dramatic.

The grain size in the consolidated powder material could not be characterized by normal metallographic techniques at magnifications as high as 1600X. Several etchants were tried, but the grain size seemed to be too fine to resolve. Therefore, the base line extruded and grain coarsened materials were prepared for scanning electron microscopy (SEM). Again, the response of the material to several standard etchants was either poor or inconsistent. The best results were obtained with a Michigan "B" etch. The base line grain size can be seen to be about 1-2μm in Fig. 2. As shown in Fig. 3, 1150°C/4 hr coarsens the grain diameter to ~5μm and 1200°C/4 hr leads to a grain size of almost 10μm. The large blocky features in these micrographs are eutectic γ' with an occasional carbide or boride, as verified by Kevex analysis.

A series of experiments was carried out to determine the effect of strain on the strain rate sensitivity parameter and to broaden the data over a wider range of strain rates to search for the sigmoidal shape typical of other materials (Ref. 17). It was immediately obvious that there were both strain and strain rate effects. Previously only three flow stresses were available over one decade of strain rate (and four m values). Now, using four specimens and four decades of strain rate, 24 flow stresses (with repeats at higher strains) are available as well as 44 m values. The step changes were carefully planned to jump up as well as down, with large as well as small changes (but all within one decade on one sample).

There were several conclusions. Previous attempts to generate such data using multiple specimens had failed due to a strain dependence. With much more data, it could be seen that the flow stress decreased slightly with strain at the high strain rates. This effect was quite pronounced in the grain coarsened material. This would strongly suggest that grain size refinement is occurring during superplastic forming in these alloys, even though the deformation temperature is below the solvus by 110°C. Figures 4 and 5 show the data for ε = 10 $\pm$ 5% and 25 $\pm$ 5%, respectively, for both the as-extruded base line and the 1150°C/4 hr coarsened state. Figures 6 and 7 indicate flow stresses for ε = 40 $\pm$ 5 and ε = 55 $\pm$ 5, respectively. These latter figures include the as-extruded base line and the 1050°C/4 hr coarsened material.

Careful examination of the full range of data indicates that since the sigmoidal character of strain rate response was found, the behavior of the 1150°C coarsened material can be matched to that of the as-extruded base line by a shift of approximately one decade in strain rates; i.e., the coarsened material

is superplastic, but at an order of magnitude lower strain rate. (On these plots, the 1050 and 1150°C coarsened materials are nearly identical.) The data are generally very well behaved when taken in ε intervals of no more than 10%. Otherwise, changes of up to 20 MPa at a given strain rate may give the appearance of scatter.

Another approach is to average the flow stress values measured at various strains at a given strain rate and plot $\bar{\sigma}$ vs $\dot{\bar{\varepsilon}}$ as in Fig. 8. The smooth curve drawn through this master plot leads to Fig. 9, a plot of the strain rate sensitivity parameter, m, as a function of strain rate for the as-extruded powder. now it can be seen that for superplasticity ($m \geq .3$), the allowable strain rate range for as-extruded PWA 1056 is from 2.5×10^{-2} to 5% S^{-1} or 1.5 to 300% min^{-1}. This is consistent with industrial practice which is generally in the range 3% to 40% min^{-1}. Coarser grain sizes than 1-2μm would mean a shift to lower strain rates (~0.1 in strain rate for ~3X in grain size).

3.2 Rapidly Solidified Structures

Arc melted buttons were prepared in a partial pressure of argon and gradually solidified over a 1-3 min period from bottom to top to avoid shrinkage. These buttons are made from 50-400g and contain fine microstructures which are relatively easily homogenized. Forming specimens are then cut out either parallel or transverse to the columnar grain growth pattern with an aspect ratio of 2:1 for height:width. For repeated compressive yield strength measurement, an aspect ratio of from 3:1 to 4:1 is used. This gives stability to the forming specimen, but leads to a finite zone without major end effects for yield stress measurements. A modification of IN-100 (no vanadium) was homogenized prior to forming. This alloy was the focus of an extension of the strain rate sensitivity testing which had been completed for the consolidated powder. A typical strain rate change sequence is shown in Fig. 10. The collective results are shown in Fig. 11. The data are truly remarkable in that they are very well behaved (with little strain dependence) over four decades of strain rate, and are decidedly linear. The m value is 0.22. This is very close to the critical value of 0.3 for superplasticity. Additionally, no cracking was observed during the strain rate sensitivity testing out to 60% reduction in height at 1204°C.

The effect of strain rate on dynamically recrystallized grain size is clearly shown in Figs. 12 and 13 where the grain size is seen to gradually be refined as the average strain rate is increased from 0.006% S^{-1} to 6% S^{-1}. A factor of 10^3 increase in strain rate brings about a factor of 10 decrease in grain diameter, namely from 1 mm to 0.1 mm. These results seem to indicate little static recrystallization or grain growth after forming during a furnace cool; otherwise the grain size differences might not be so pronounced. Nonetheless, this will be checked by direct experimentation involving withdrawal of the formed specimen from the hot zone.

The lack of a dependence of flow stress on strain level and the lack of any non-linearities in the $\ln \sigma$ vs $\ln \dot{\varepsilon}$ plot for the columnar grained arc melted buttons of modified PWA 1058 (IN-100) must be a consequence of the fact that the material is constantly dynamically recrystallizing above the solvus temperature. This is in direct contrast to the powder work below the solvus, where grain size changes, although they occur to some degree, are not significant in the overall deformation behavior.

The true flow stress vs true strain is plotted in Fig. 14 for buttons of modified PWA 1058 (IN-100) at various strain rates. Note the steady character of these flow curves. A peak in true stress below a strain of 10% would indicate the onset of dynamic recrystallization at relatively low strain levels. The evolution of the recrystallized grain structure was monitored for the exact conditions set forth in Fig. 14 at strain levels of 15, 30, 45 and 60%. These results are shown in Figs. 15-17. Note that the dynamically recrystallized grain structure is considerably finer at 12.5% S^{-1} vs 5 x 10^{-3} % S^{-1} and that the recrystallization process has just barely begun at 15% strain at 5 x 10^{-3} % S^{-1}, whereas it has progressed considerably further at the same 15% strain level at the selected strain rate of 12.5% S^{-1}. Although the grain refinement is remarkable, the data of Fig. 14 are entirely consistent with those of Fig. 11, namely $m \simeq 0.22$. Further grain size refinement is apparently required for superplasticity.

Starting with a columnar grained arc melted button of modified 1058, an attempt was made to significantly impact the grain size by cooling through the gamma prime solvus temeprature during forming. The rams, buttons and forming specimen were soaked at 1204°C to obtain initial isothermal conditions. Forming was initiated at 0.33% S^{-1} (20% min^{-1}). At that rate 60% strain only takes about 4.4 min (due to a slowdown to maintain constant true strain rate). After 1 min, the furnace was turned off. The temperature declined almost immediately and dropped about at the rate of 20°C/min. After 2.5 min into the deformation cycle (40% strain, see Fig. 18), the temperature dropped below the gamma prime solvus.

Figures 19 and 20 show how the stress varied with strain and with temperature. Figure 20 shows an undercooling of about 28°C before the flow stress truly escalates. The experiment seemed to work as planned. No cracking occurred. Without preconditioning the microstructure by straining above the solvus, the specimen would have surely cracked below the solvus at a 20% min^{-1} strain rate. Note the outstanding grain size refinement indicated in Fig. 21. The initial grain structure can still be seen in the dead zone near the Lucalox loading platens (no lubrication was used in these experiments). The final grain size characteristics and the strain rate sensitivity remain to be determined. The structure looks extremely interesting and promising.

A significant step forward was made in obtaining more massive high cooling rate cast alloys when it was demonstrated that 1200-1500 gram buttons could be obtained by a skull melting technique using electron beam processing. Three to four 400 gram buttons can be made by conventional arc processing, and these can be combined into one large button using electron beam melting. These large buttons were melted twice to ensure chemical homogeneity. A gradual power down (1-3 min) was used after the melting cycle to minimize any residual porosity and to maximize the opportunity for the flotation of oxide inclusions. The ingot structure was fully workable in the form of a 70 gram 2/1 aspect ratio specimen under heat treatment and working conditions established for 200-400 gram buttons. The 3, 20 and 70 gram formed specimens all showed no evidence of cracking. It is highly encouraging that a 23X scale-up in weight and volume was obtained in MOD 1058 and the 1013-1058 blended alloy without difficulty. A further scale-up may be required before tensile ductility can be measured in the formed condition.

An initial attempt was made to prepare some material by drip melting. A vacuum induction melt was prepared by heating drop cast bars of modified IN-100 in a recrystallized Al_2O_3 crucible. A recrystallized Al_2O_3 protection tube with a 1.0 mm internal diameter served as an orifice and was held in place with high purity alumina cement. A frequency of 350 k Hz was used to heat a tantalum susceptor around the charge. Fibrous zirconia was used to separate the hot zone from the cold zone, where a water cooled copper mold was positioned. At a vacuum of 10^{-4} Torr, the mold was rapidly heated from 1300 to 1500°C. The entire melt dripped out in about 4 min. The crucible and the as-cast ingot are shown in Fig. 22. The copper mold was 5 cm in diameter by 10 cm in length with a 1.2 cm diameter tapered hole. The temperature rise in the copper mold was only 60°C. A ceramic shell mold with an orifice of 1.5 mm (dia) produced about the same result.

The dendrites were extremely fine, as indicated in Fig. 23. The primary spacing at the center is consistent with a cooling rate of 10^3 °C/s. This had been estimated previously in Table I for a structure similar to a drop casting. The dendrite size did not vary markedly with location in the ingot from bottom to center. Figure 24 shows that there was a small amount of porosity near the top end, as well as larger dendrites. Figure 24 also shows the eutectic pools and carbide particles trapped between the dendrites at the top end of the ingot.

The ingots did not appear to have surface connected porosity, so an attempt was made to Hot Isostatically Press (HIP) one without "canning". The conditions used were 1120°C/2 hr/100 MPa. The resulting microstructures are shown in Figs. 25 and 26. The as-HIP grain size is 0.3 mm; that is to be compared with an initial grain size in the homogenized arc melted buttons of 5 mm x 0.5 mm dia. In fact, the initial grain size will now be comparable to that obtained <u>after</u> forming of the arc melted buttons. Figure 26 shows the grain boundary structure,

the lack of any trace of dendrites through most of the ingot and a small bit of residual porosity. Apparently this was surface connected. Figure 27 shows the "canning" approach (evacuated and degassed stainless steel) which was successfully used for a second ingot.

A considerable effort was made to assess the formability of the drip melted product. The temperature-strain rate combinations attempted are shown in Fig. 28. The temperatures ranges from 1175 to 1200°C and the strain rates attempted were 0.05% S^{-1} to 15% S^{-1}. None of these specimens were cracked externally, but internal flaws were noted in all but the 1175°C case. (This was quite repeatable.) This is not considered to be a useful condition due to the lack of recrystallization, see Fig. 29. 1175°C might work at a higher strain rate, however.

The presence of only internal cracking can be a sign of inadequate initial breakdown. Therefore the test was repeated at 1200°C with an initial strain rate of only 1% min^{-1} (vs 3% min^{-1} previously). As shown in Fig. 30, after 20% engineering strain, the strain rate was stepped up to 10% min^{-1}, and again after an engineering strain of 40% had been reached, the strain rate was jumped to 100% min^{-1}. The specimen showdd no signs of internal or external cracking.

The grain size is shown in Fig. 31 to be unremarkable. The flow stress data of Fig. 30 are entirely consistent with Fig. 11. The drip cast behaves the same as the arc melted buttons. Both can be formed above the solvus, if one is careful about initial breakdown, without the presence of superplasticity (although it is enticingly close).

These ingots appeared to be reasonably sound in about 50% of the attempts to drip melt. Most of the problems could be avoided by slight modifications in the process. Further experimentation is required to find the optimum combination of parameters to assure a reproducible process. The most significant problem seems to be a nonuniformity in as-cast grain size. This is due to a lack of a constant fill rate, which in turn is dependent upon heating rate, changes in metallostatic head pressure and the geometry relationship between orifice and chill mold. Other processes, such as the use of a uniformly heated melt or LPPS should also be investigated as alternatives to drip melting.

3.3 Single Crystals

PWA 1444 was selected as a reasonably well understood model high strength single crystal alloy. The composition of this alloy as well as others used in this phase of the program is given in Table II. The initial objective was to impose 10% strain below the solvus temperature to avoid dynamic recrystallization and to assess the influence of the stored energy on subsequent plastic flow properties. Up to 10% strain was introduced at 1190°C without difficulty. It was observed that a slight drop in yield strength at room temperature occurred

Table II

Nominal Cast Nickel Alloy Chemistries
for Workability Studies (wt %)

Type	Al	Ti	Cr	Co	Mo	V	Zr	C	B	W	Cb
1056	5.0	4.3	12	18.0	3.2	0.8	0.06	0.07	0.02	-	-
Mod. 1058	5.0	4.3	12.4	18.5	3.2	-	0.03	0.07	0.015	-	-
1444	5.0	2.0	9.0	-	-	-	-	0.05	0.03	12	1.0

after forming, possibly due to the significantly coarsened precipitated γ'. An attempt to resolution at 1245°C could not be done reproducibly without recrystallization. Partial resolutioning at 1235°C did result in a small volume fraction of coarse γ' which prevented any recrystallization. Rapid cooling preserved the bulk of the fine secondary γ' structure and resulted in a room temperature yield strength of 1000 MPa vs a base line of 965 MPa.

It has been noted that as little as 10% prestrain before a high temperature heat treatment can lead to recrystallization in the single phase γ regions which can occur due to a temperature in excess of the bulk γ' solvus, or even the local γ' solvus temperature within the dendrite cores. These regions are lower in aluminum and titanium due to microsegregation. It may be desirable to homogenize rather than simply solutionize such alloys to generate a more nearly uniform response to high temperature heat treatment. The degree of residual microsegregation after a 4 hr solution heat treatment at 1288°C has a pronounced effect on the gamma prime particle size distribution. Increasing the time to 24 hr almost eliminates the variable precipitate morphology, and a full 72 hr in this tungsten bearing alloy is required to fully homogenize crystals grown at 150°C/cm and 25 cm/hr. This may be an important treatment prior to working and resolutioning for optimum strength.

Another, perhaps simpler approach for obtaining substructure strengthening in high strength superalloys was to attempt the introduction of 5 to 10% plastic strain significantly below the γ' solvus temperature. If this could be done without buckling or kinking, substructure might be introduced without significant γ' particle size coarsening, thus obviating the need for a re-solutioning heat treatment and the risk of recrystallization. As indicated in Table III, this approach has led to significant improvements in post formed yield strength at both 20°C and the important temperature of 595°C (typical root attachment or disk rim temperature).

These studies were carried out to 5 and 10% plastic strain at both 890 and 990°C in the three high symmetry orientations: <001>, <110> and <111>. The results are rather remarkable. Note that the base line yield strengths are reproducible to at least $\pm$ 1.8%. At the 890°C condition, even 5% strain leads to a 26% improvement in <100> and a 57% increase in <111> yield strength at 595°C. The 10% strain values are again improved (except for <110>) relative to the 5% increments. In every case up to 10% strain, working led to substructure strengthening. (This had not been the case at 1190°C.) The 10% strain experiment at 890°C did result in a kink for the <111> crystal. The <110> results should be repeated at 890°C since the hardening does not appear to be monotonic strain.

Table III

Substructure Strengthening in Hot Worked PWA 1444 Crystals

Orient.	Starting Condition*		Def. Cycle		After Deformation		Y.S. Increase	
	0.2% Y.S. (ksi)		Strain	Temp	0.2% Y.S. (ksi)		(%)	
	20°C	595°C	(%)	(°C)	20°C	595°C	20°C	595°C
[001]	140.6	131.3	5	990	155.2	150.4	10.4	14.5
"	138.8	131.7	10	990	160.0	154.7	15.3	17.5
"	138.1	131.6	5	890	174.9	166.0	26.6	26.1
"	143.5	136.2	10	890	187.7	177.3	30.8	30.2
"	141.3	132.0	15	890	179.4	168.4	27.0	27.6
[011]	159.8	139.5	5	990	174.5	175.0	9.2	25.4
"	159.1	137.9	10	990	169.1	172.0	6.3	24.7
"	160.2	141.1	5	890	197.6	193.5	23.3	37.1
"	157.0	136.4	10	890	177.7	179.2	13.2	31.4
"	164.2	144.2	13+	890	120.3	101.2	(-)	(-)
[111]	166.1	115.0	5	990	209.2	167.1	26.0	45.0
"	164.2	112.5	10	990	221.6	182.5	35.0	62.2
"	165.4	116.0	5	890	222.5	182.6	34.5	57.4
"	162.7	112.0	10	890	208.0	192.2	27.8	71.6
"	160.9	114.1	15	890	219.8	205.6	36.9	80.2

*1288°C/4 hr/AC + 1080°C/4 hr/AC + 870°C/32 hr/AC; Aspect Ratio = 2:1

+ test planned for 15% strain discontinued due to onset of failure

Testing was extended to 15% prestrain in all three orientations. As indicated in Table III, further strengthening occurred in <111>, almost no change in <001> and a drop (due to specimen failure) in the <011> orientation. The <111> strengthening is quite impressive with a 37% improvement in yield strength at room temperature and an 80% improvement in compressive yield strength at 595°C.

3.4 Acknowledgement

Technical progress on this program is due largely to the efforts of Robert E. Doiron of PWA/CPD/MERL. His consistent dedication to careful planning and accurate measurement has kept the work progressing at a rapid pace and at a sustained high level of quality.

FIG. 1

Ln STRESS vs ln STRAIN RATE PLOT FOR AS EXTRUDED AND GRAIN COARSENED PWA 1056 CONSOLIDATED POWDER BILLET

T_F = 1080°C, e = 15 ± 10%

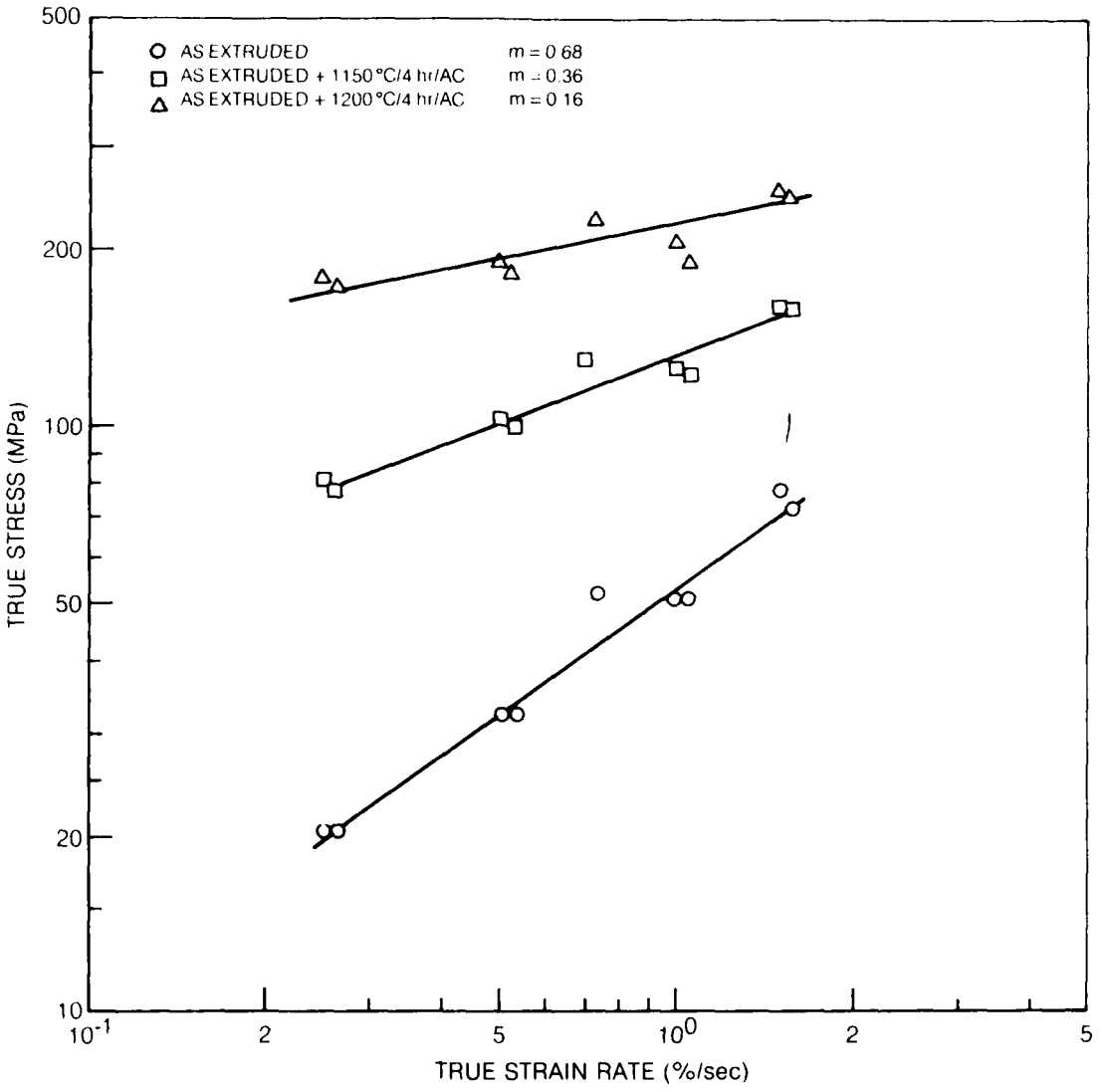

81-8-3-1

FIG. 2

SEM PHOTOS SHOWING GRAIN SIZE IN AS EXTRUDED PWA 1056

a)

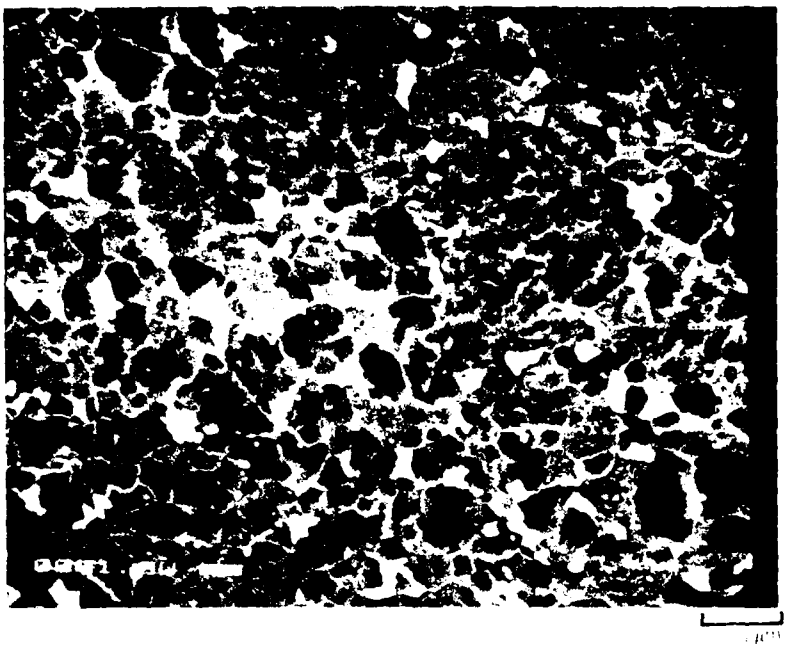

b)

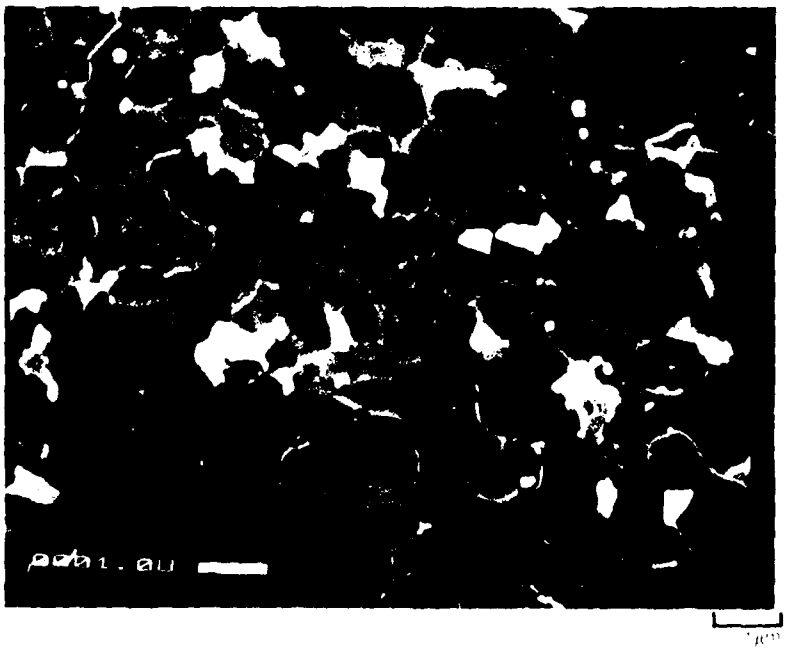

81 12 8 10

SEM PHOTOS SHOWING GRAIN SIZE IN HEAT TREATED PWA 1056

a) 1150C/4 hr/AIR COOL, 1200 C/4 hr/AIR COOL

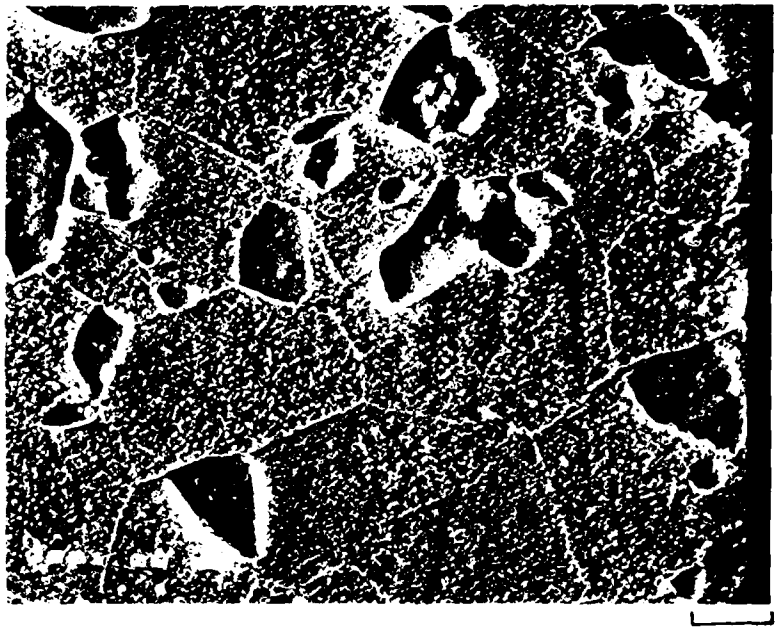

b) 1200C/4 hr/AIR COOL

FIG. 4

Ln STRESS vs ln STRAIN RATE PLOT WITH EXTENDED STRAIN RATE RANGE FOR PWA 1056 EXTRUDED BILLET; TAKEN FOR $\epsilon = 10 \pm 5\%$

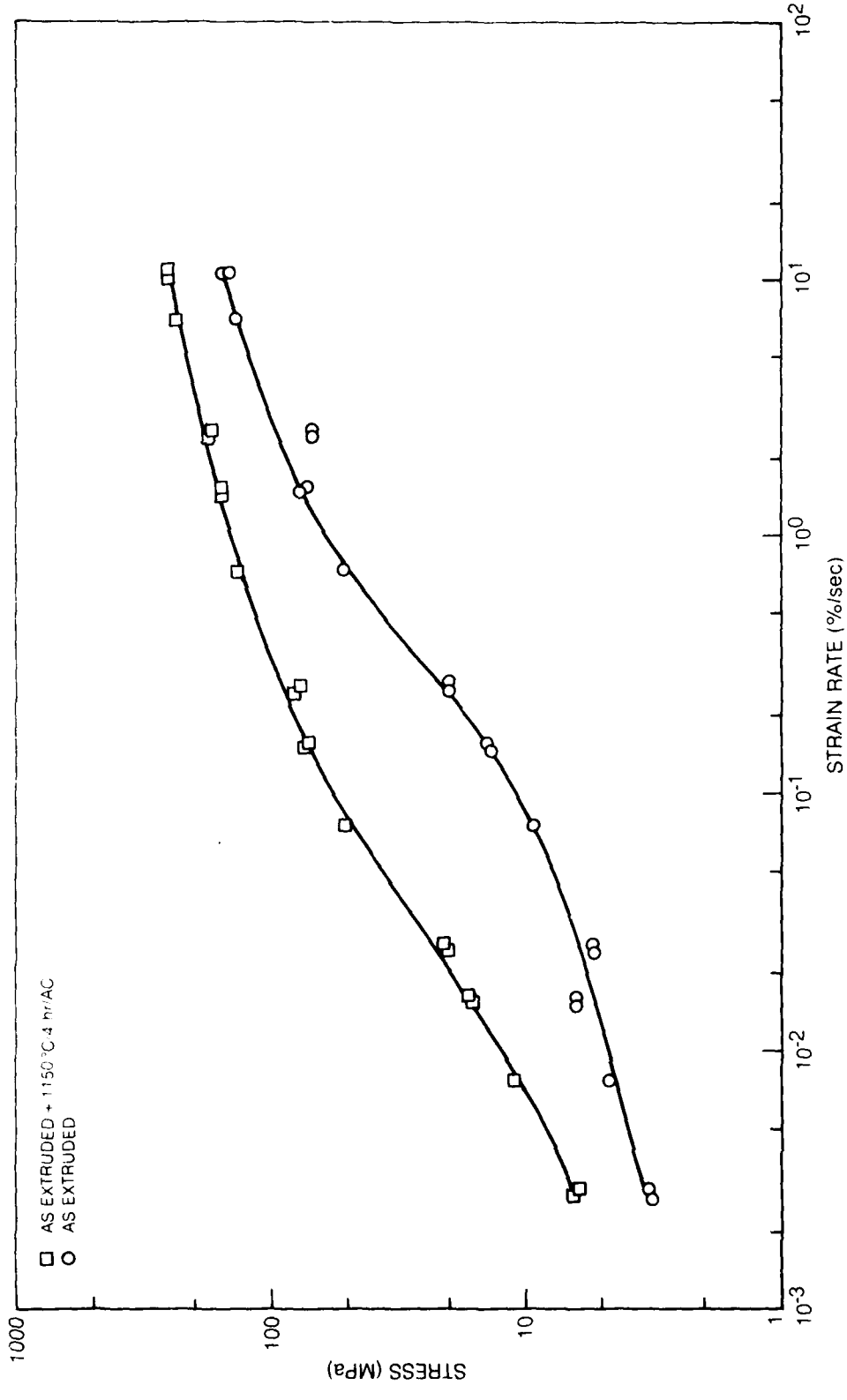

81-8-3-2

FIG. 5

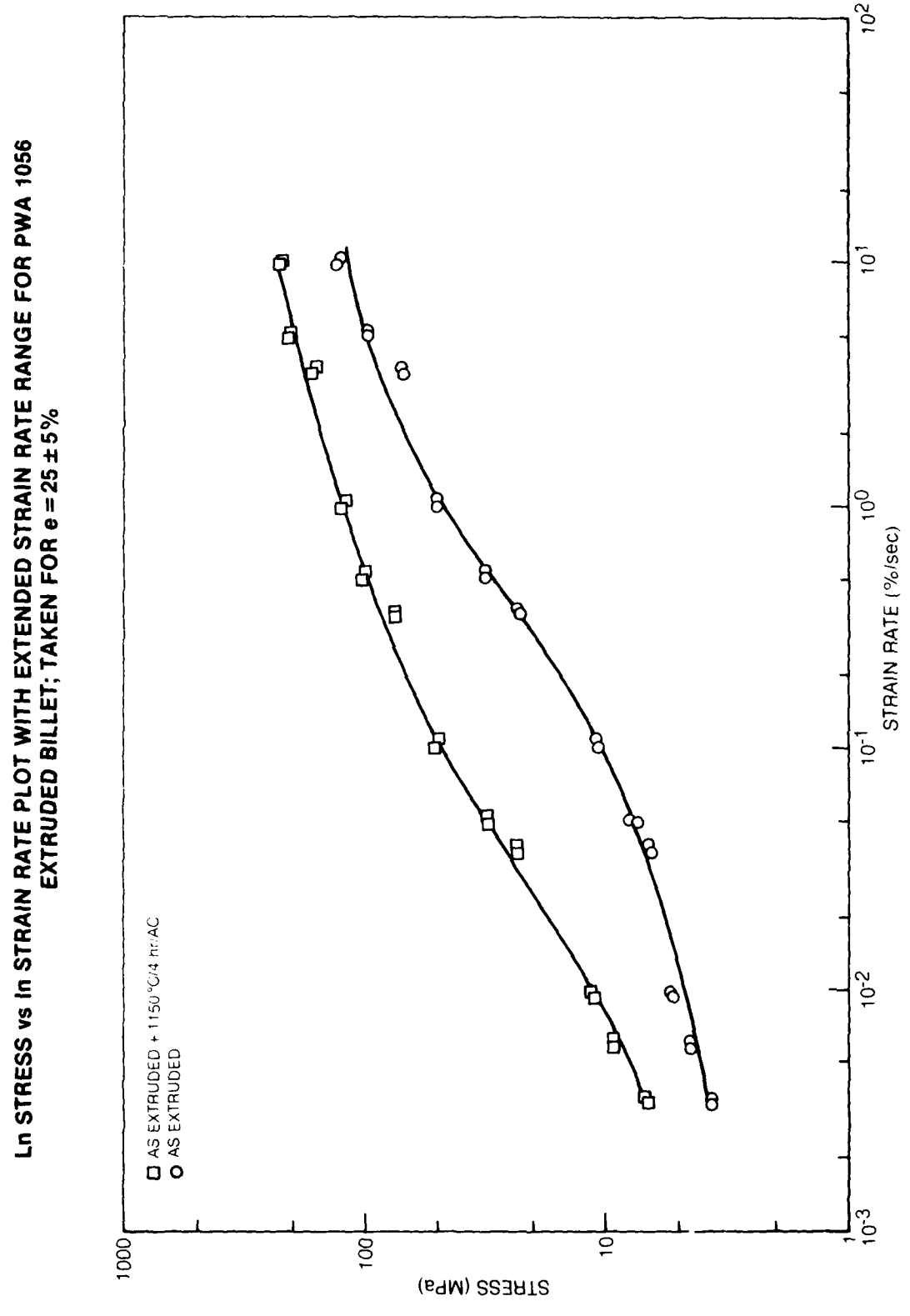
Ln STRESS vs ln STRAIN RATE PLOT WITH EXTENDED STRAIN RATE RANGE FOR PWA 1056
EXTRUDED BILLET; TAKEN FOR e = 25 ± 5%
AS EXTRUDED + 1150°C/4 hr/AC
AS EXTRUDED
STRESS (MPa)
1000
100
10
1
STRAIN RATE (%/sec)
10^{-3}
10^{-2}
10^{-1}
10^{0}
10^{1}
10^{2}

81-8-3-3

FIG. 6

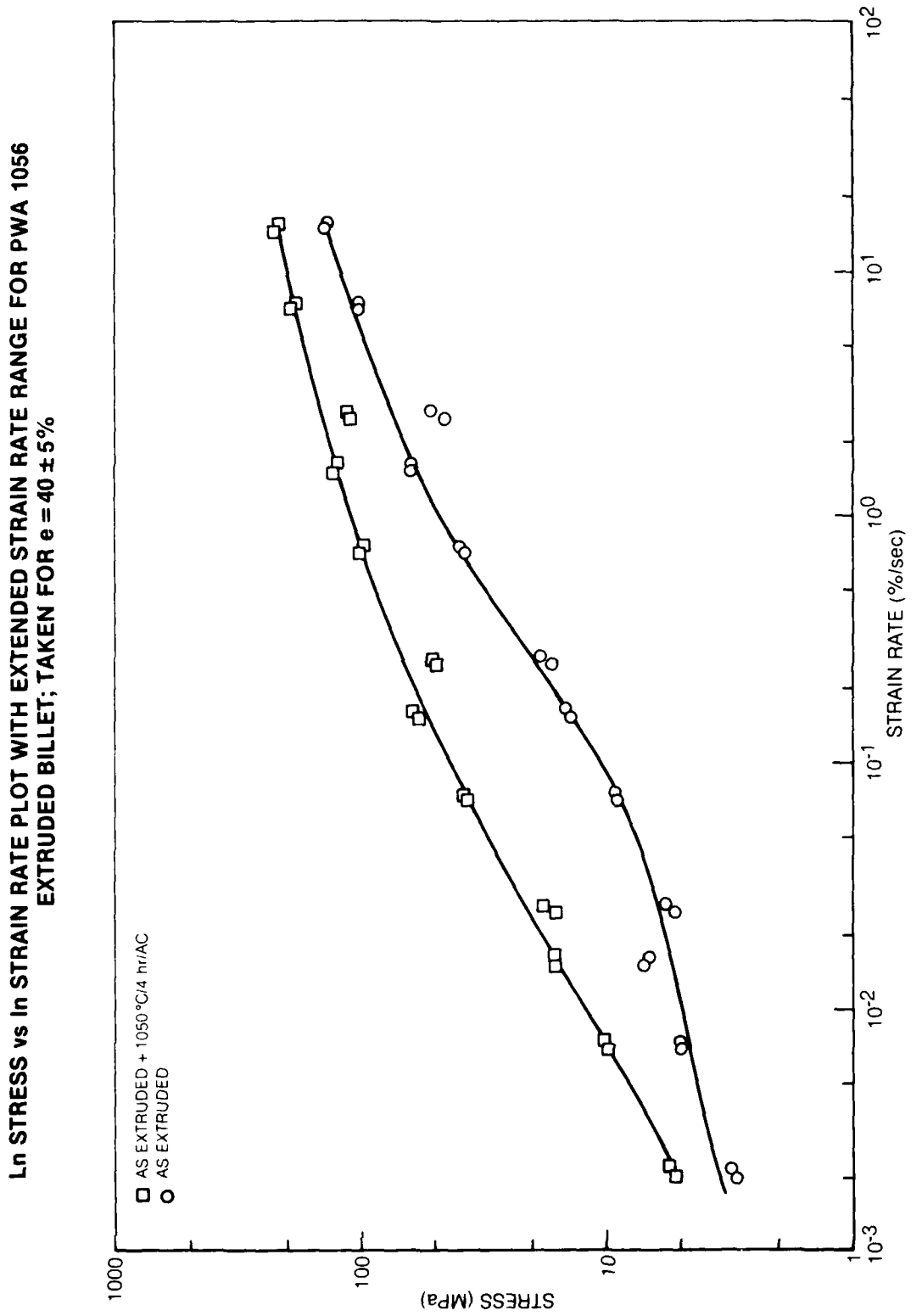
Ln STRESS vs ln STRAIN RATE PLOT WITH EXTENDED STRAIN RATE RANGE FOR PWA 1056
EXTRUDED BILLET; TAKEN FOR e = 40 ± 5%
AS EXTRUDED + 1050 °C/4 hr/AC
AS EXTRUDED
STRESS (MPa)
1000
100
10
1
STRAIN RATE (%/sec)
10^{-3}
10^{-2}
10^{-1}
10^{0}
10^{1}
10^{2}

81-8-3-4

FIG. 7

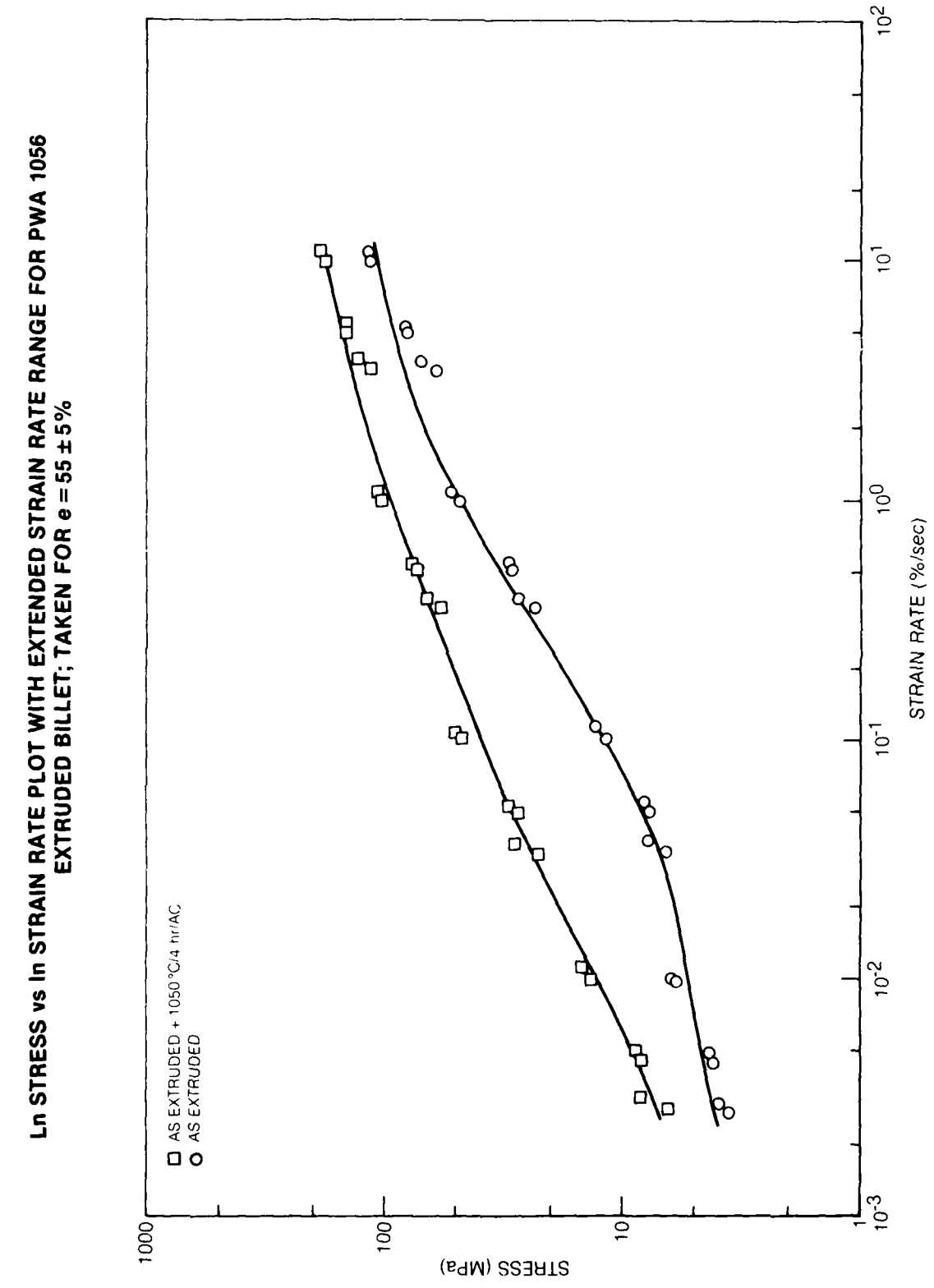
Ln STRESS vs ln STRAIN RATE PLOT WITH EXTENDED STRAIN RATE RANGE FOR PWA 1056
EXTRUDED BILLET; TAKEN FOR e = 55 ± 5%
AS EXTRUDED + 1050°C/4 hr/AC
AS EXTRUDED
STRESS (MPa)
1000
100
10
1
STRAIN RATE (%/sec)
10^{-3}
10^{-2}
10^{-1}
10^{0}
10^{1}
10^{2}

81-8-3-5

FIG. 8

LN STRESS VS LN STRAIN RATE WITH TRUE FLOW STRESS AVERAGED AT VARIOUS STRAIN LEVELS

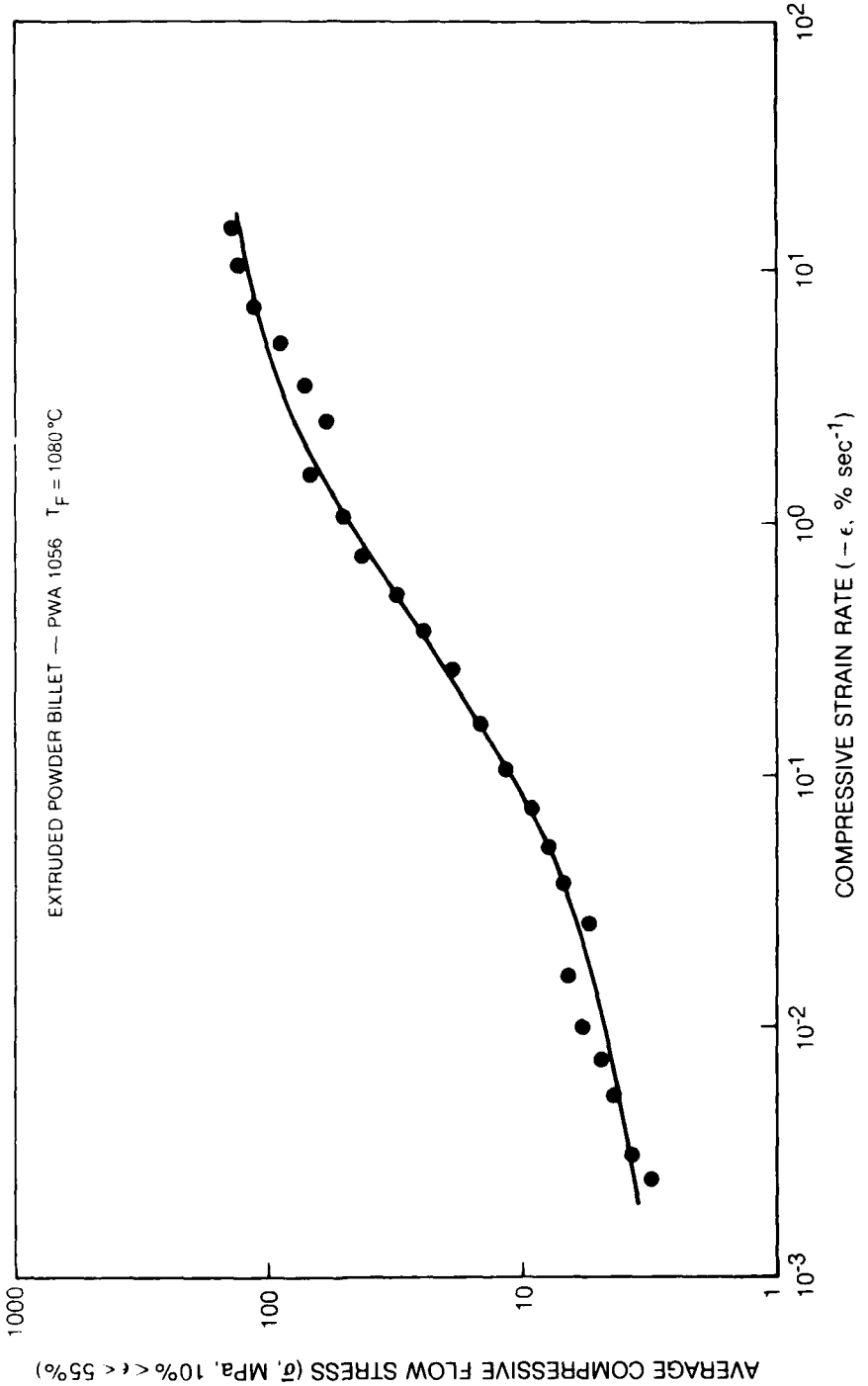

81-12-8-2

FIG. 9

STRAIN RATE SENSITIVITY PARAMETER, M, AS DETERMINED FROM THE SMOOTH CURVE IN FIG. 8 VS LN STRAIN RATE

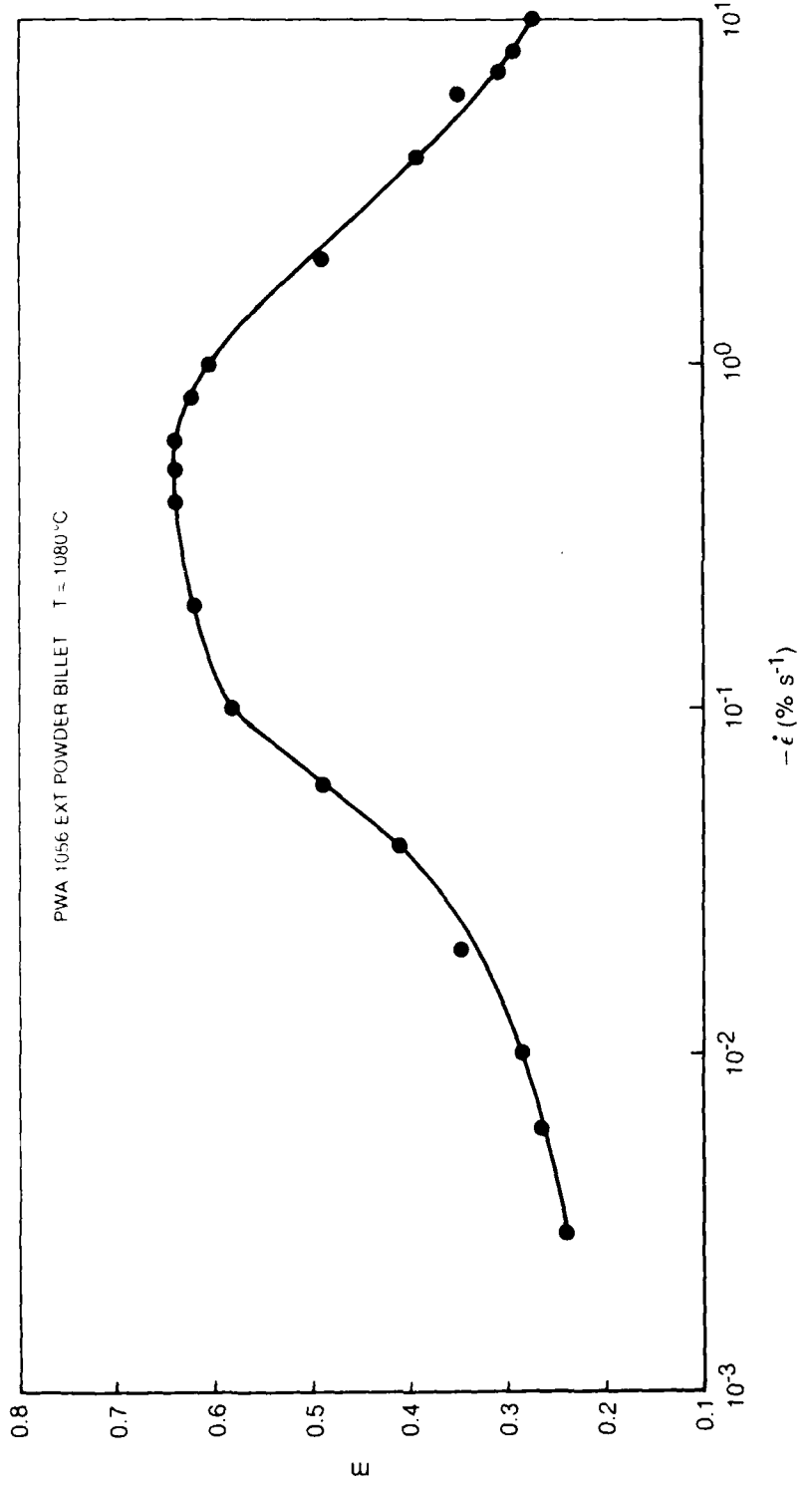

81-12-8-3

DETAILED PLAN AND EXAMPLE OF STRAIN RATE SCHEDULE FOR THE RANGE $\dot{\epsilon} = 0.25$ TO 1.5% S^{-1}

$T_F = 1204\,°C$
1204 °C/24 hr/FFC

ϵ	0-5	5-10	10-15	15-20	20-25	25-30	30-35	35-40	40-45	45-50	50-55	55-60	(%)
$\dot{\epsilon}$	0.7	1.5	0.25	0.5	1.0	0.35	0.7	1.5	0.25	0.5	1.0	0.35	(% S^{-1})

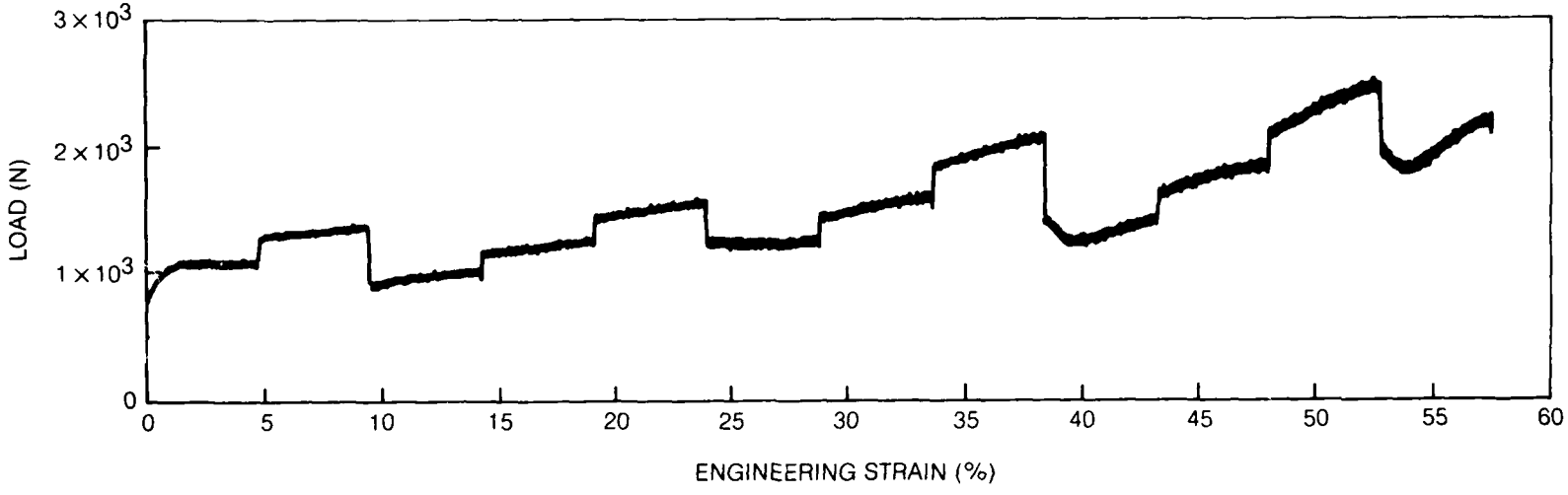

FIG. 10

Ln STRESS vs *ln* STRAIN RATE PLOT WITH EXTENDED STRAIN RATE RANGE FOR MODIFIED IN100

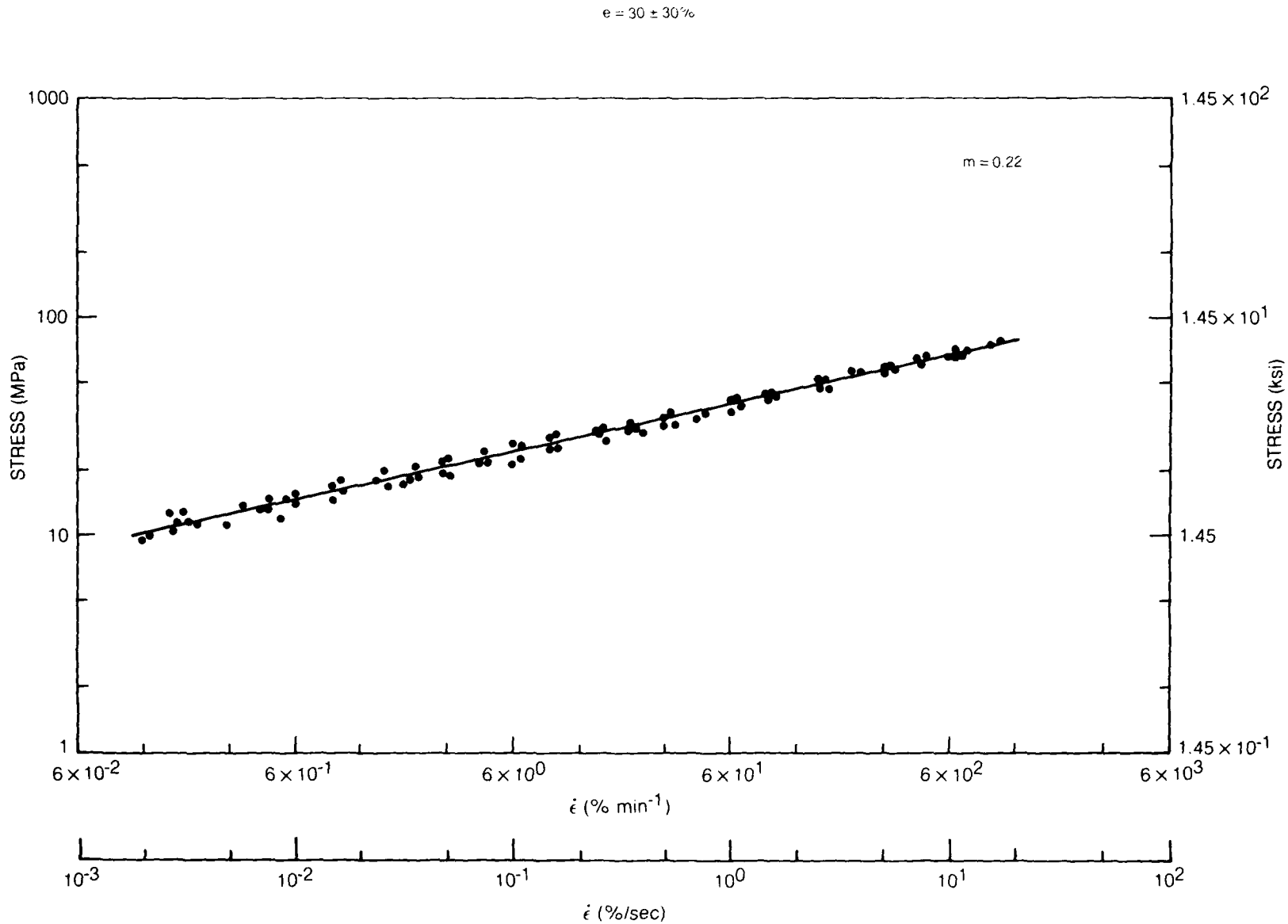

FIG. 11

81-8-3-7

FIG. 12A

MODIFIED IN100 UPSET TO 60% REDUCTION AT $<\dot{\varepsilon}> = 0.006\%\ S^{-1}$

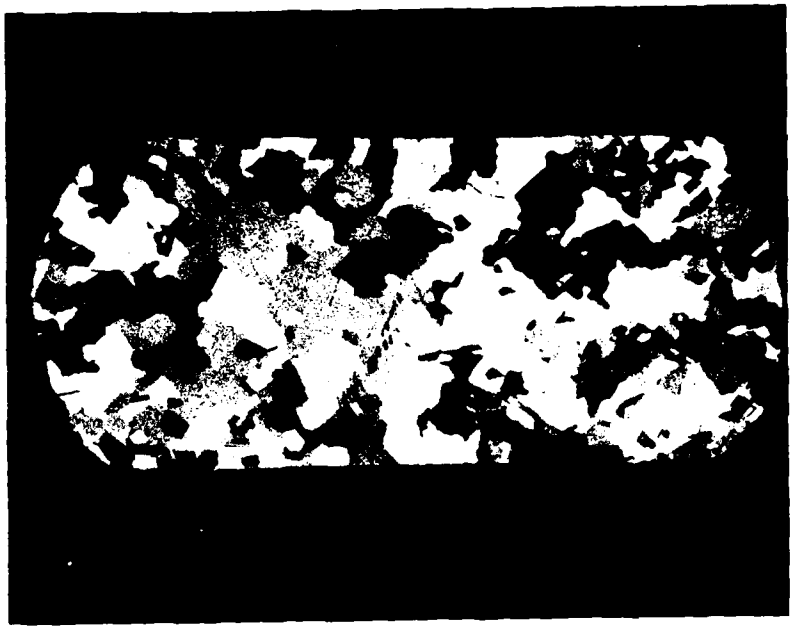

FIG. 12B

MODIFIED IN100 UPSET TO 60% REDUCTION AT $<\dot{\varepsilon}> = 0.06\%\ S^{-1}$

81-8-3-8

FIG. 13A

MODIFIED IN100 UPSET TO 60% REDUCTION AT $<\dot{\varepsilon}>$ =0.6% S^{-1}

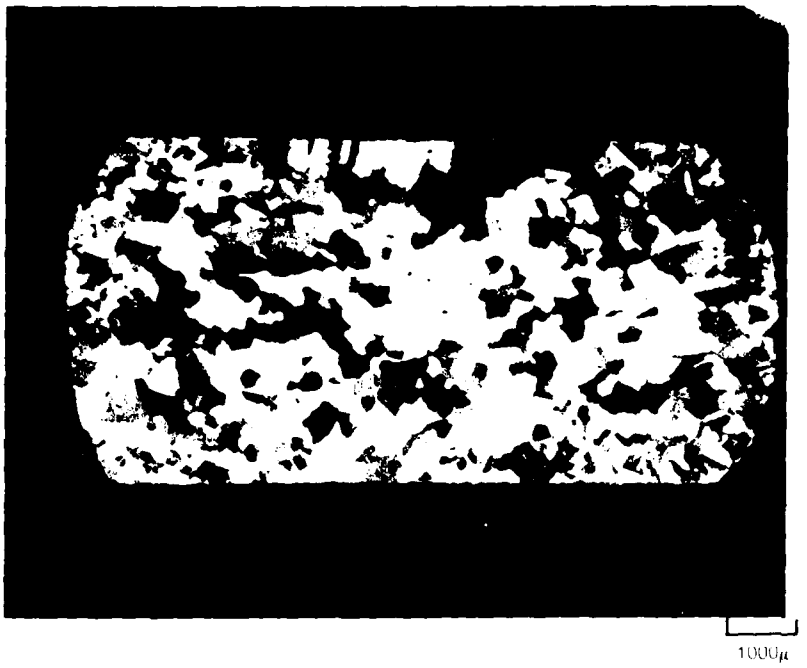

FIG. 13B

MODIFIED IN100 UPSET TO 60% REDUCTION AT $<\dot{\varepsilon}>$ =6.0% S^{-1}

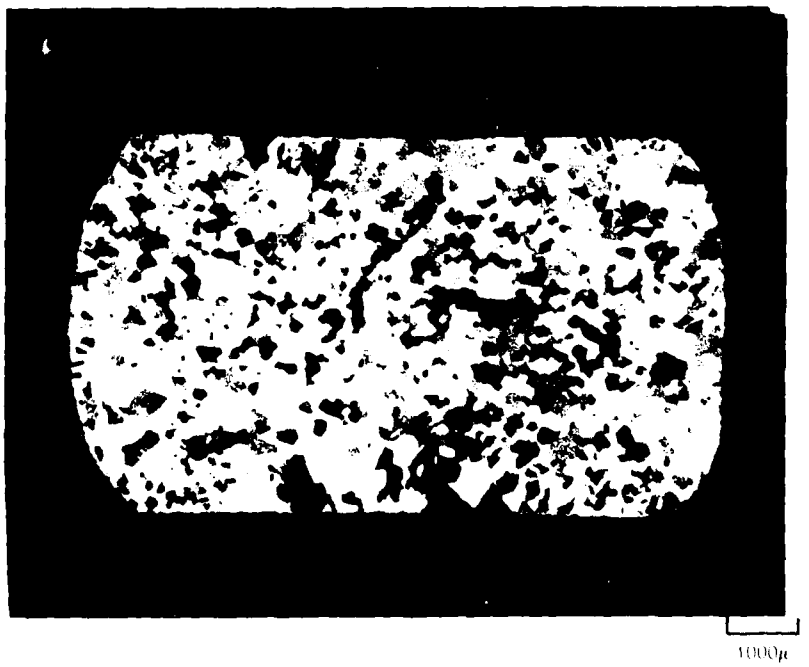

81-8-3-9

FIG. 14

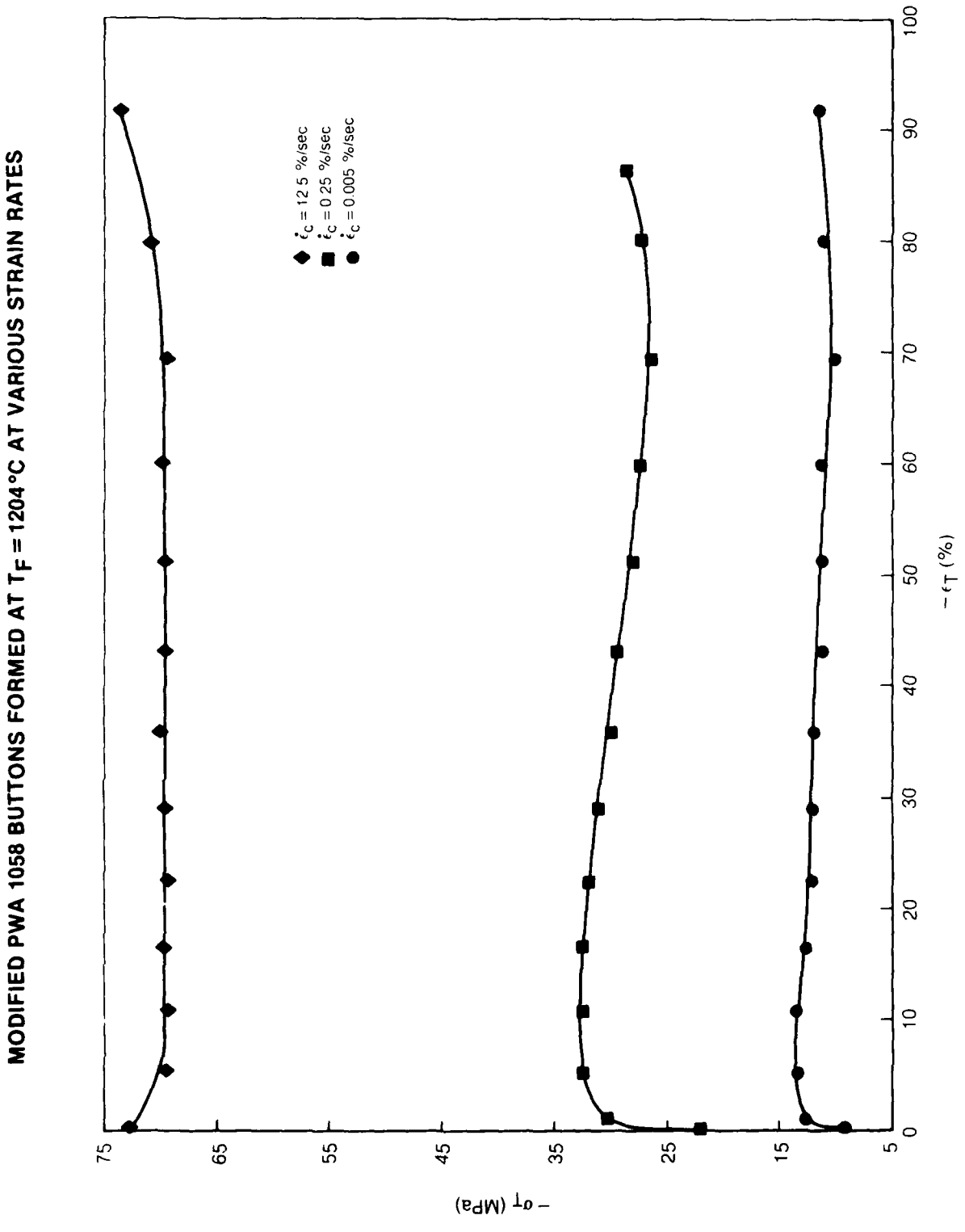
MODIFIED PWA 1058 BUTTONS FORMED AT T_F = 1204°C AT VARIOUS STRAIN RATES
$\dot{\epsilon}_C$ = 12.5 %/sec
$\dot{\epsilon}_C$ = 0.25 %/sec
$\dot{\epsilon}_C$ = 0.005 %/sec
$-\sigma_T$ (MPa)
75
65
55
45
35
25
15
5
$-\epsilon_T$ (%)
0
10
20
30
40
50
60
70
80
90
100
81-12-8-4

FIG. 15

LONGITUDINAL SECTIONS OF MODIFIED IN100 FORMED AT 1204°C AT 5×10^{-3} % s^{-1} TO THE INDICATED STRAIN LEVELS

(a) 15%

(b) 60%

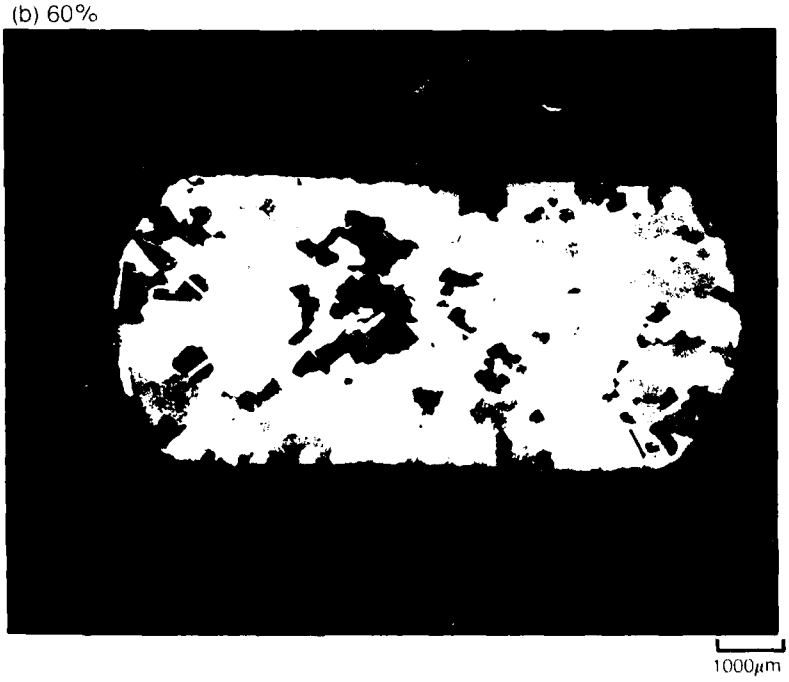

81-12-8-13

FIG. 16

LONGITUDINAL SECTIONS OF MODIFIED IN100 FORMED AT 1204°C AT 2.5×10^{-1} % s^{-1} TO THE INDICATED STRAIN LEVELS

(a) 15%

(b) 60%

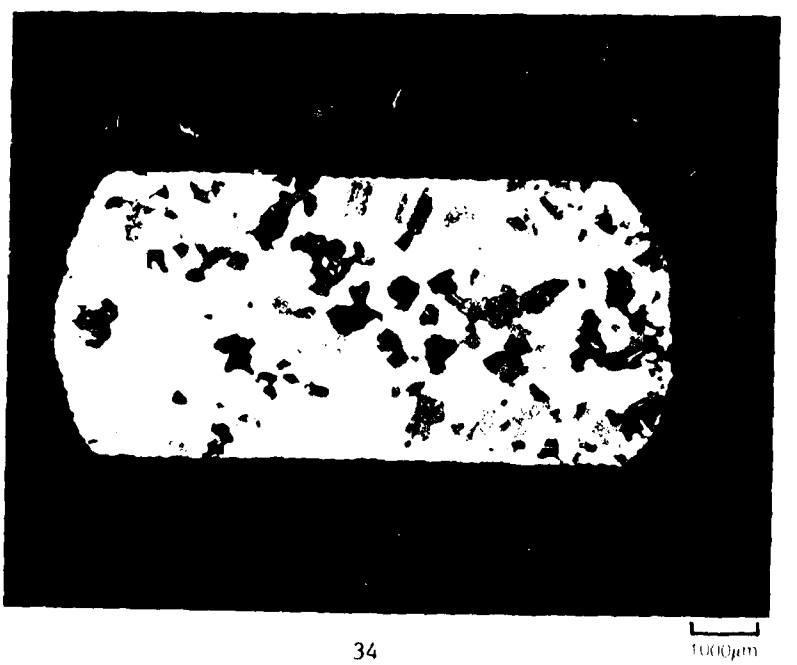

81-12-8-14

FIG. 17

LONGITUDINAL SECTIONS OF MODIFIED IN100 FORMED AT 1204°C AT 12.5% s^{-1} (750% min^{-1}) TO THE INDICATED STRAIN LEVELS

(a) 15%

(b) 30%

81-12-8-15

LONGITUDINAL SECTIONS OF MODIFIED IN100 FORMED AT 1204°C AT 12.5% s^{-1} (750% min^{-1}) TO THE INDICATED STRAIN LEVELS

(c) 45%

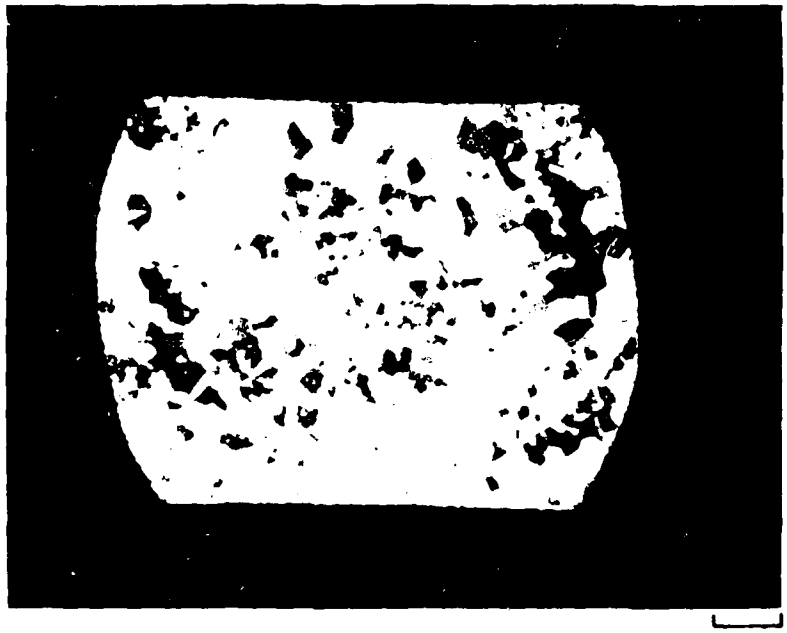

(d) 60%

FIG. 18

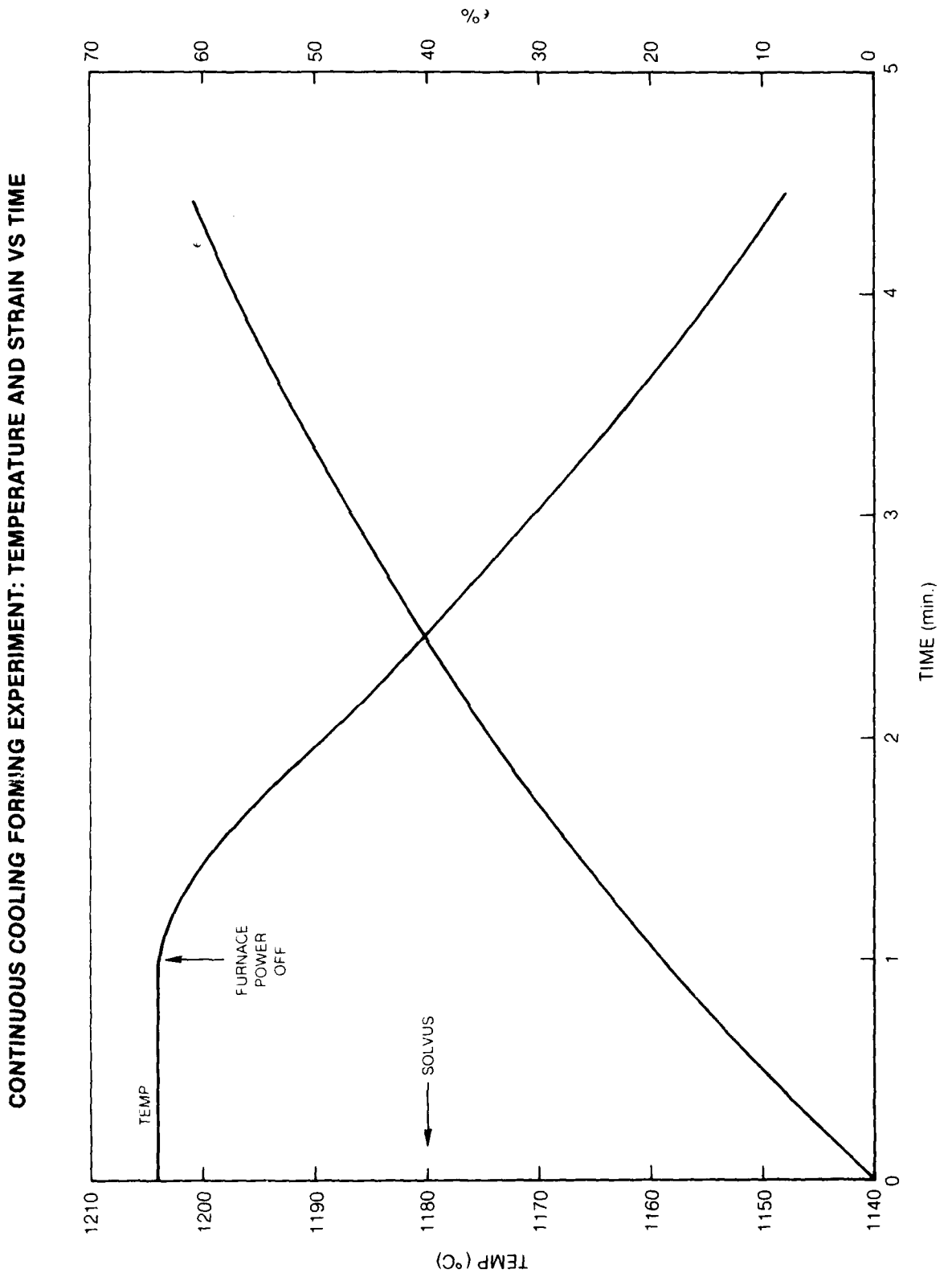
CONTINUOUS COOLING FORMING EXPERIMENT: TEMPERATURE AND STRAIN VS TIME
TEMP (°C)
%'
TIME (min.)
1210
1200
1190
1180
1170
1160
1150
1140
70
60
50
40
30
20
10
0
0
1
2
3
4
5
TEMP
FURNACE POWER OFF
SOLVUS
81-12-8-5

FIG. 19

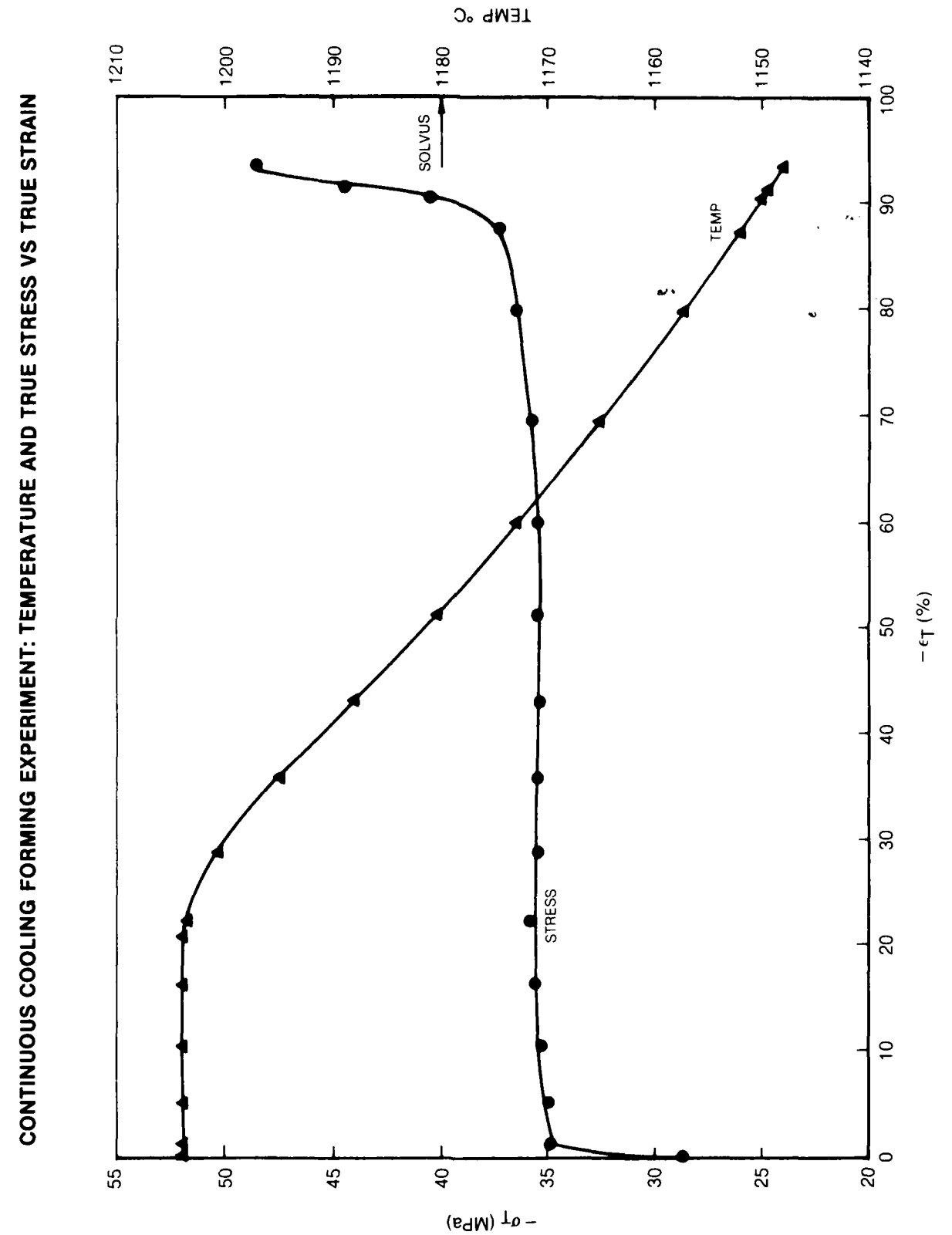
CONTINUOUS COOLING FORMING EXPERIMENT: TEMPERATURE AND TRUE STRESS VS TRUE STRAIN
TEMP °C
1210
1200
1190
1180
1170
1160
1150
1140
SOLVUS
TEMP
STRESS
55
50
45
40
35
30
25
20
$-\sigma_T$ (MPa)
100
90
80
70
60
50
40
30
20
10
0
$-\epsilon_T$ (%)
81-12-8-6

FIG. 20

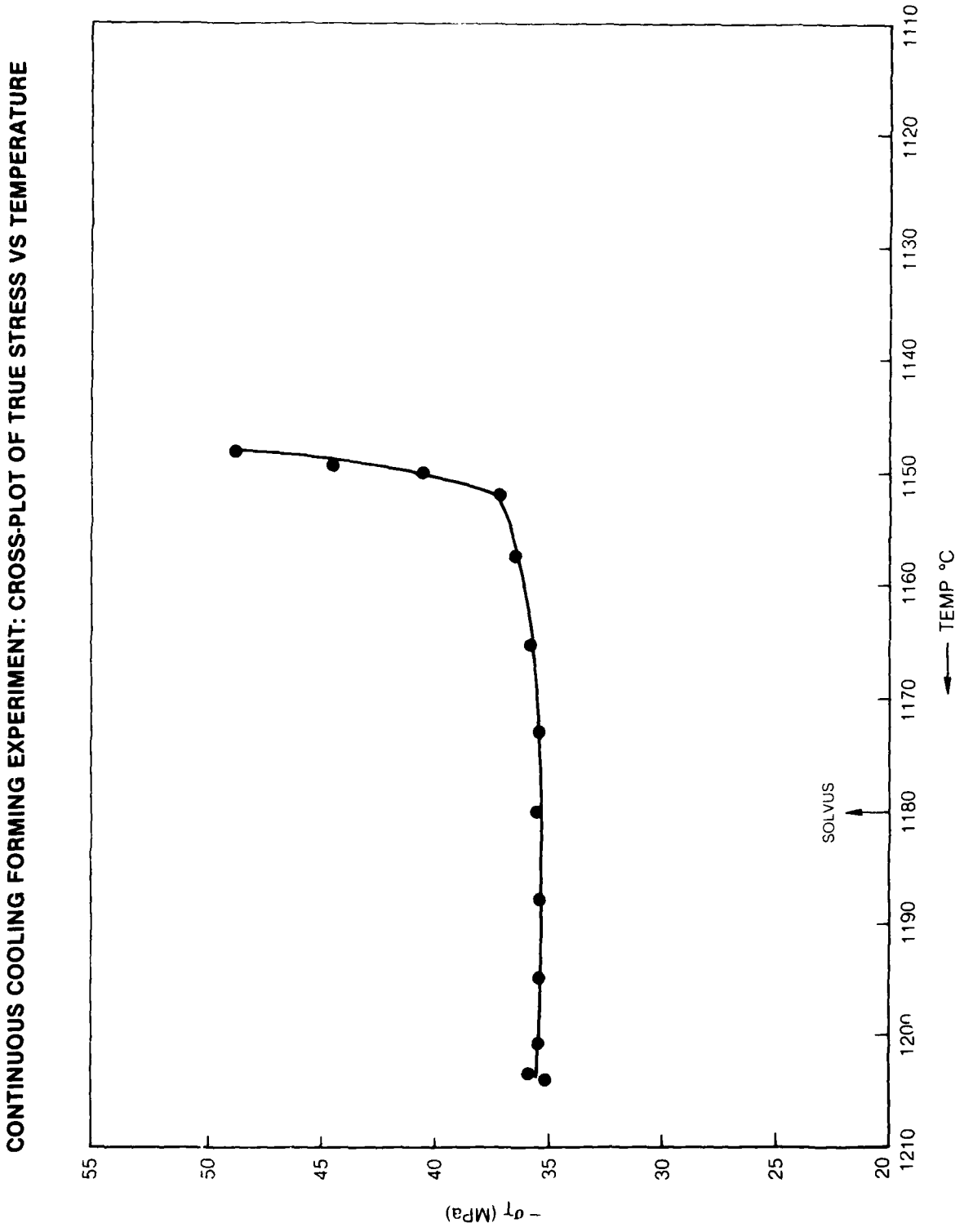
CONTINUOUS COOLING FORMING EXPERIMENT: CROSS-PLOT OF TRUE STRESS VS TEMPERATURE
55
50
45
40
35
30
25
20
$-\sigma_T$ (MPa)
1110
1120
1130
1140
1150
1160
1170
1180
1190
1200
1210
TEMP °C
SOLVUS
81-12-8-7

FIG. 21

LONGITUDINAL SECTION AT 60% STRAIN FROM MODIFIED IN-100 CONTINUOUS COOLING FORMING EXPERIMENT

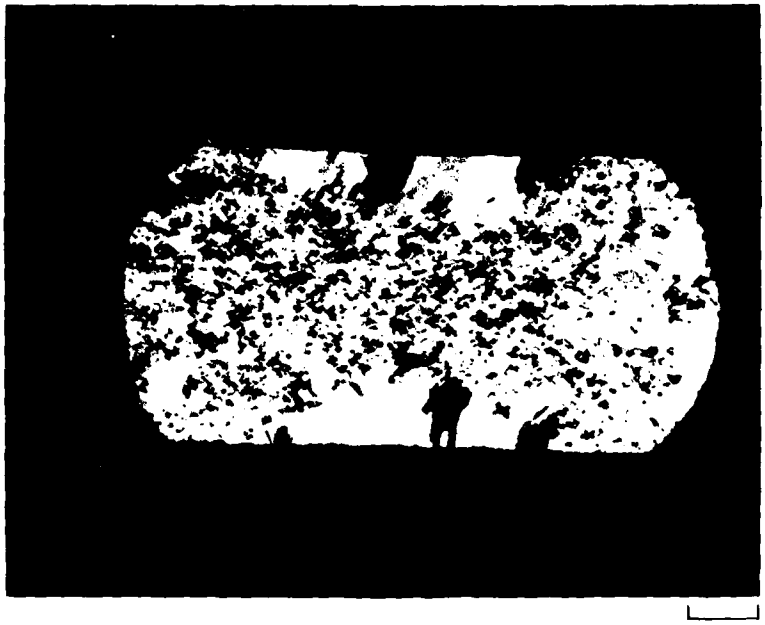

1000μm

FIG. 22A

DRIP MELTING CRUCIBLE AND ORIFICE

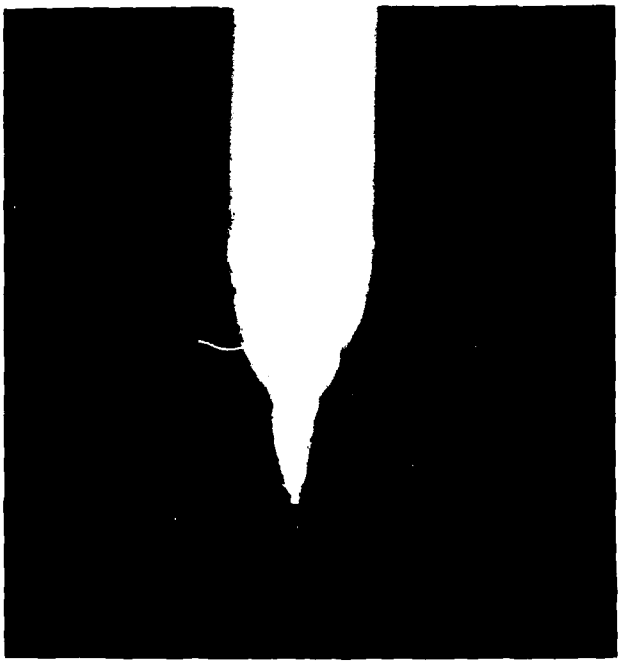

FIG. 22B

DRIP MELTED INGOT TAKEN FROM COPPER MOLD

81-8-3-10

FIG. 23A

BOTTOM SECTION OF DRIP MELTED MODIFIED IN100

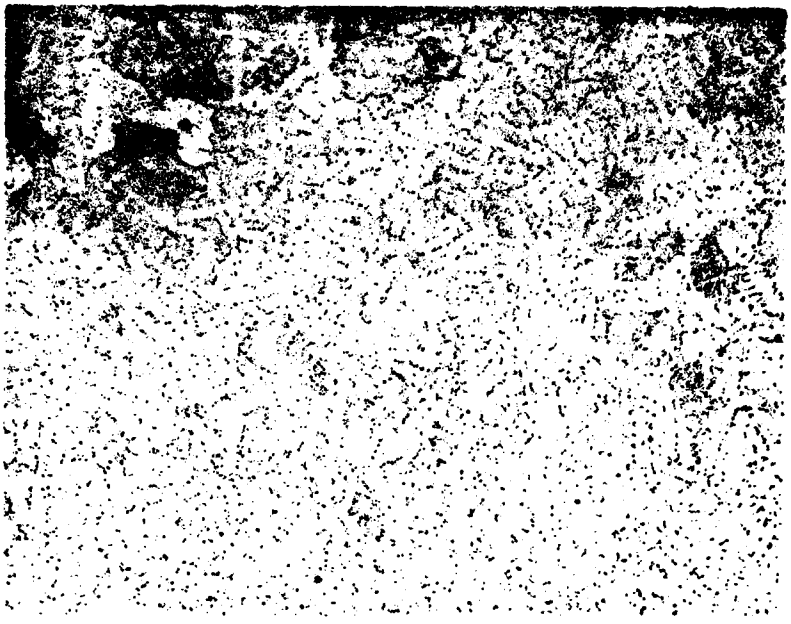

FIG. 23B

CENTER SECTION OF DRIP MELTED MODIFIED IN100

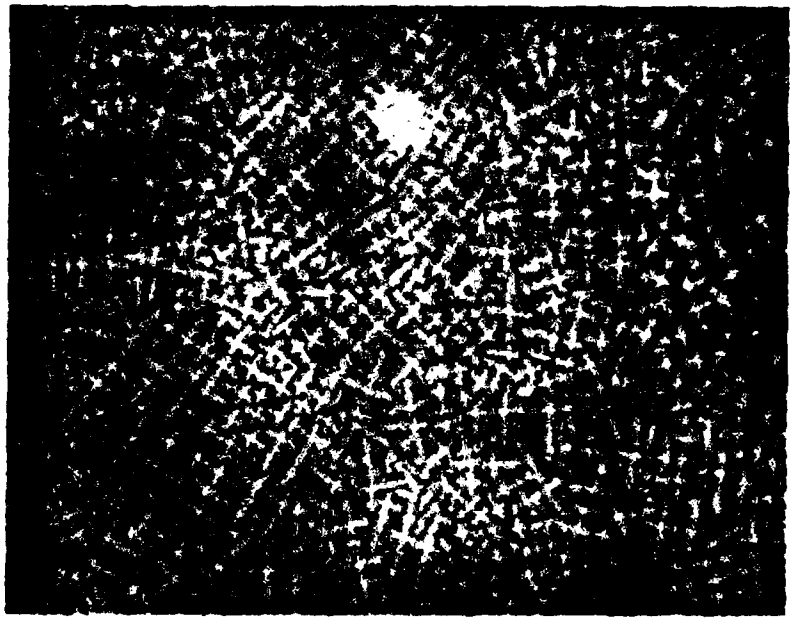

FIG. 24A

DENDRITES AND SHRINKAGE POROSITY AT TOP OF DRIP MELTED MODIFIED IN100

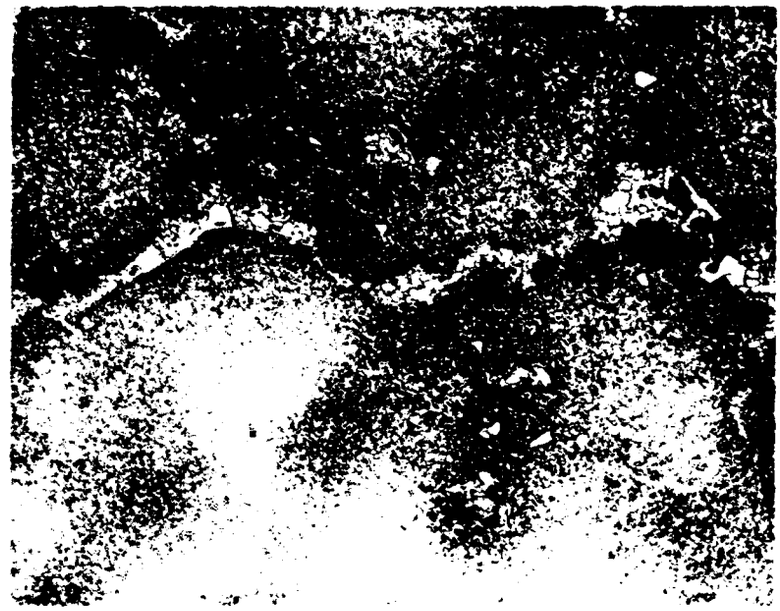

FIG. 24B

EUTECTIC AND CARBIDES AT TOP OF DRIP MELTED MODIFIED IN100

FIG. 25A

GRAINS IN DRIP MELTED MODIFIED IN100 AFTER HIP CYCLE

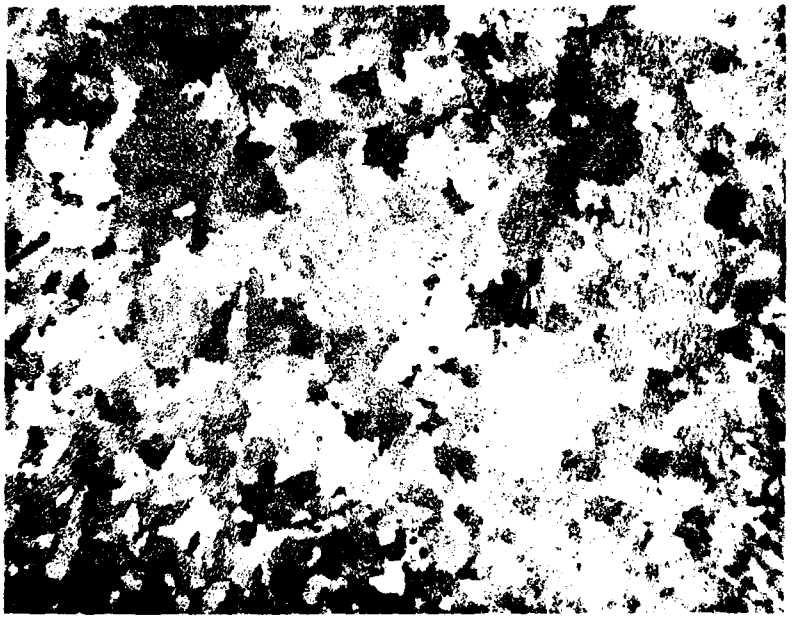

FIG. 25B

γ/γ' IN DRIP MELTED MODIFIED IN100 AFTER HIP CYCLE

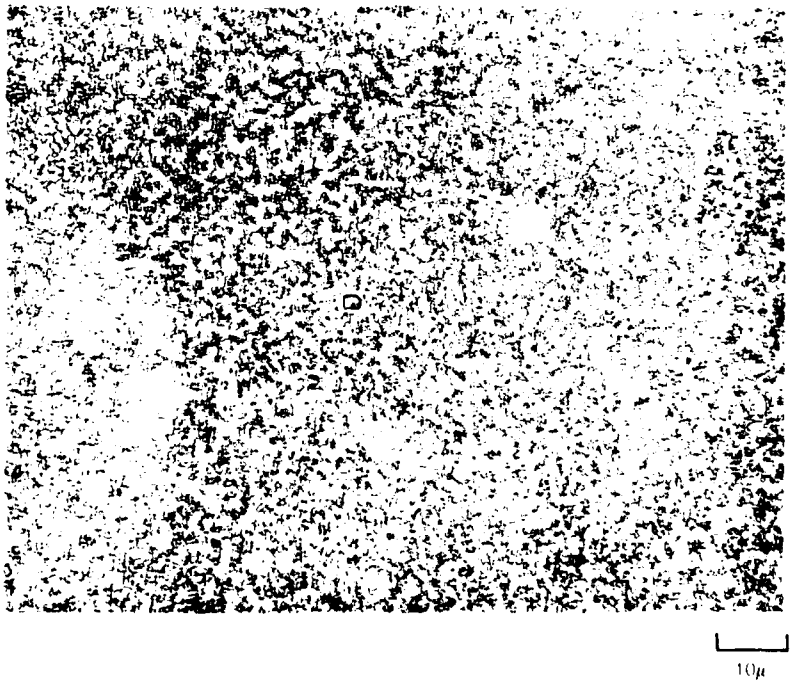

FIG. 26A

GRAIN BOUNDARIES IN DRIP MELTED MODIFIED IN100 AFTER HIP

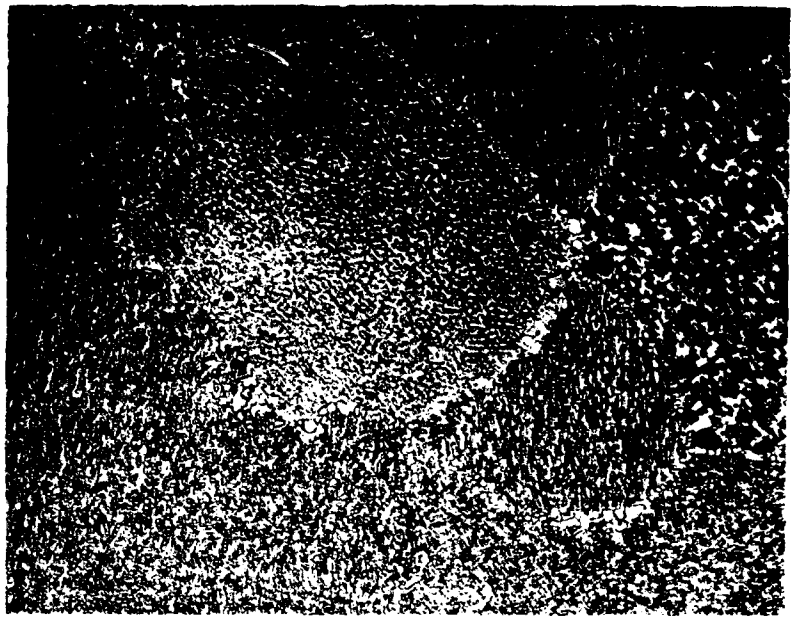

10μ

FIG. 26B

RESIDUAL POROSITY IN DRIP MELTED MODIFIED IN100 AFTER HIP (WITHOUT CONTAINER)

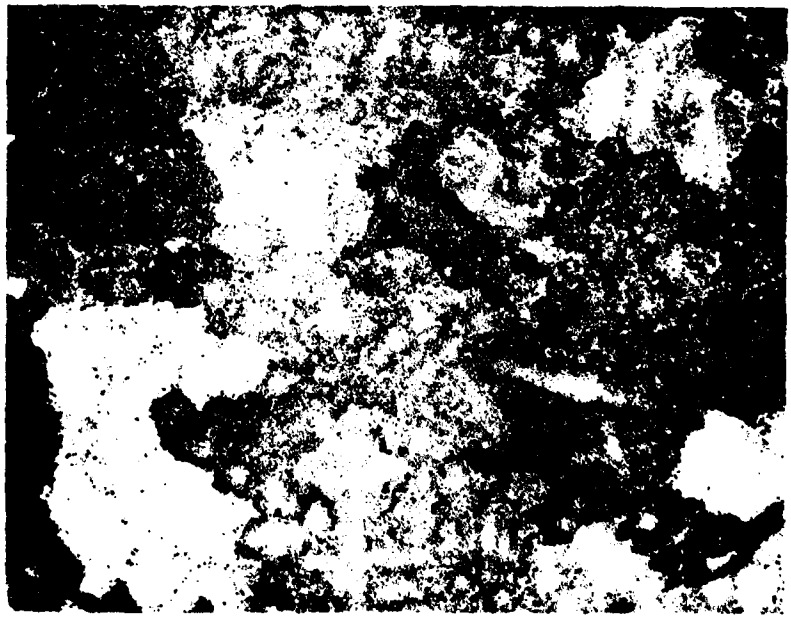

100μ

81-8-3-14

FIG. 27

DRIP MELTED INGOT CANNED IN STAINLESS STEEL PRIOR TO HIP CYCLE

2.5 cm

81-8-3-15

FIG. 28

FORMING CURVES FOR DRIP CAST IN-100

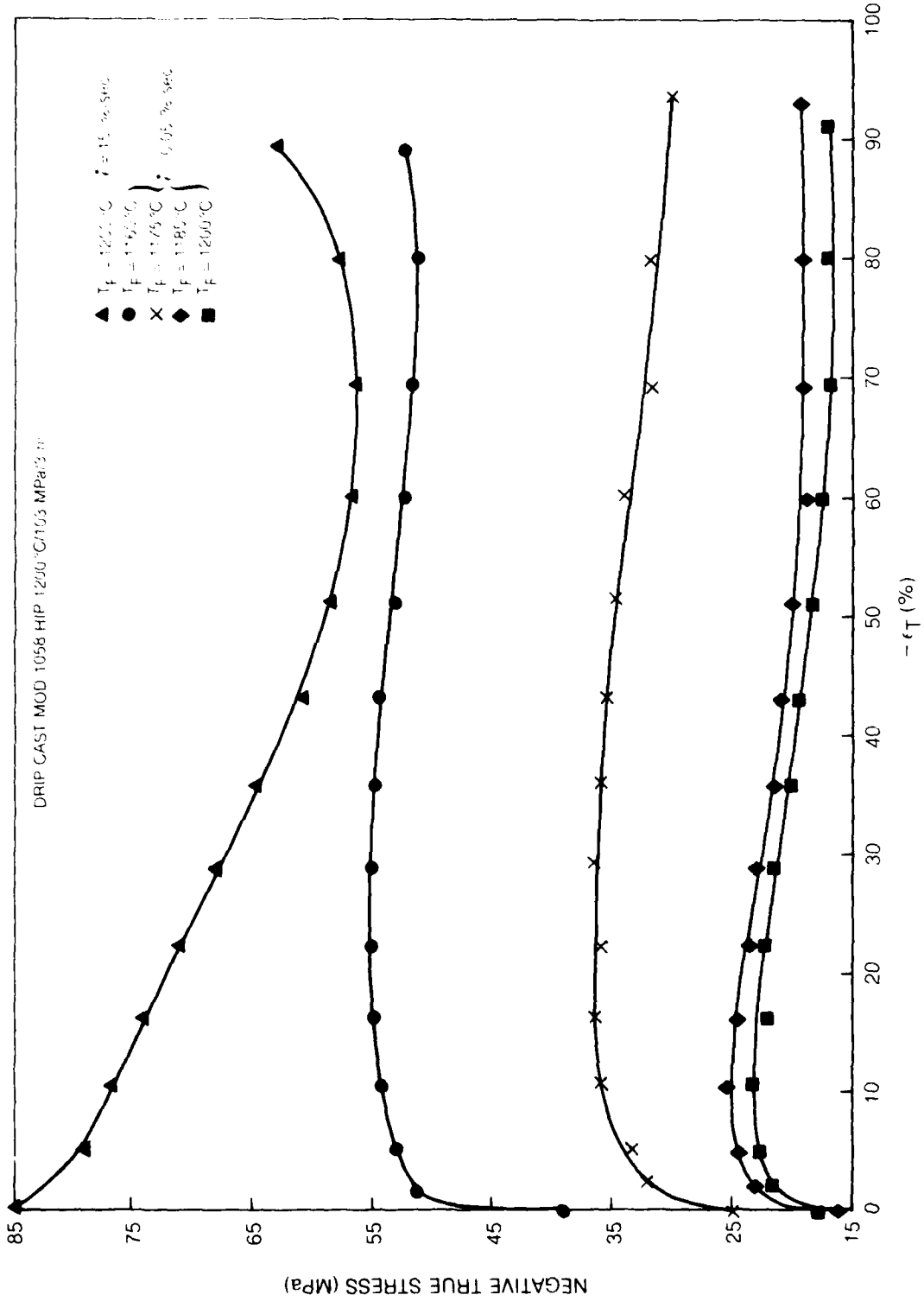

81-12-8-8

DRIP + HIP MODIFIED IN-100 BEFORE AND AFTER FORMING AT 1175°C AT 0.05% s^{-1}

NOTE LACK OF RECRYSTALLIZATION

(a) BEFORE

1000μm

(b) AFTER

1000μm

FIG. 29

FIG 30

FORMING/STRAIN RATE SENSITIVITY/TEST OF DRIP + HIP IN-100

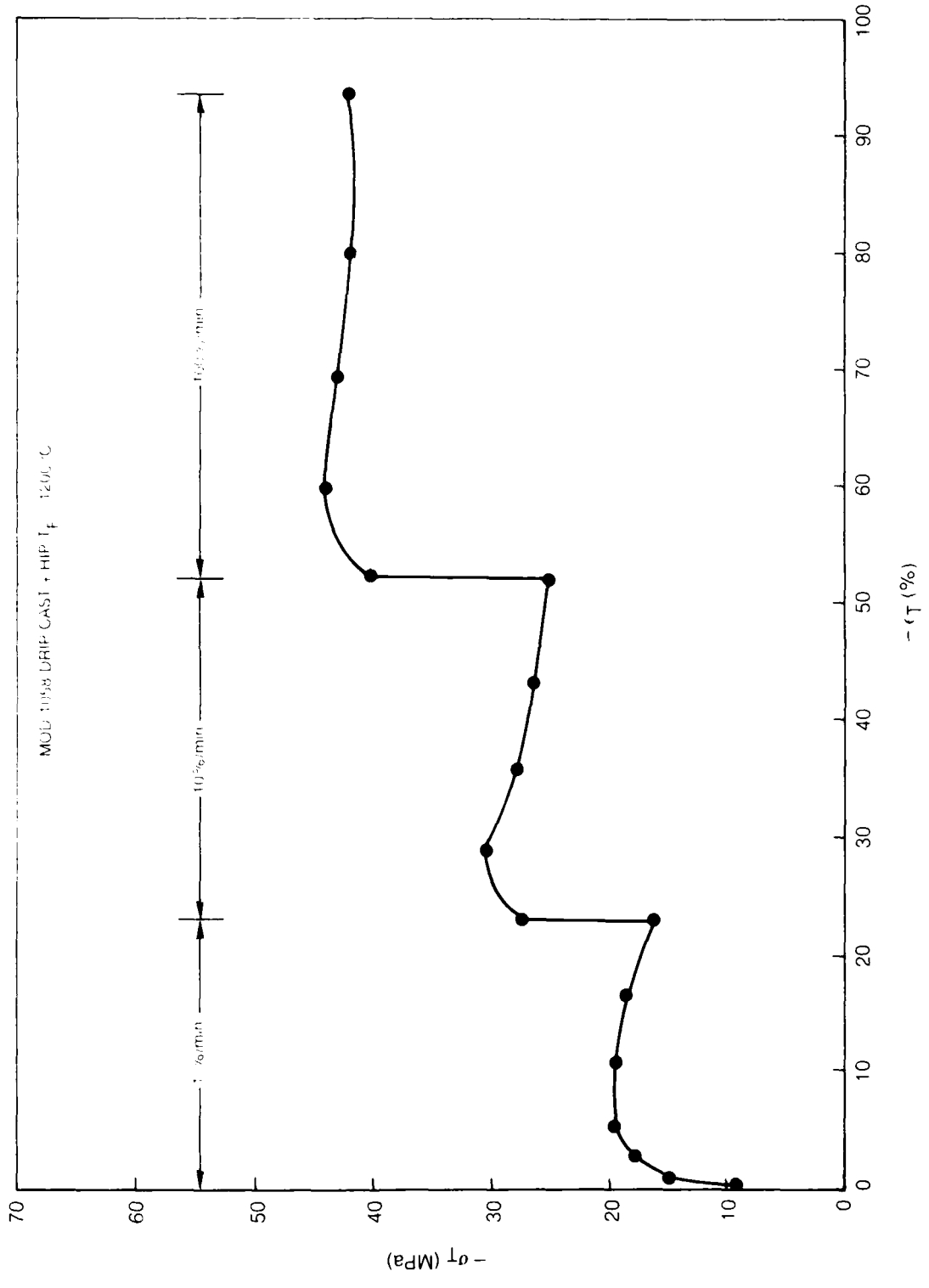

81-12-8-9

LONGITUDINAL SECTION (i.e. COMPRESSIVE STRESS AXIS IS VERTICAL) FOR DRIP + HIP MODIFIED IN-100 FORMED AT 1200°C INITIALLY AT 1% min^{-1} WITH TWO 10X JUMPS ENDING AT 100% min^{-1} STRAIN RATE

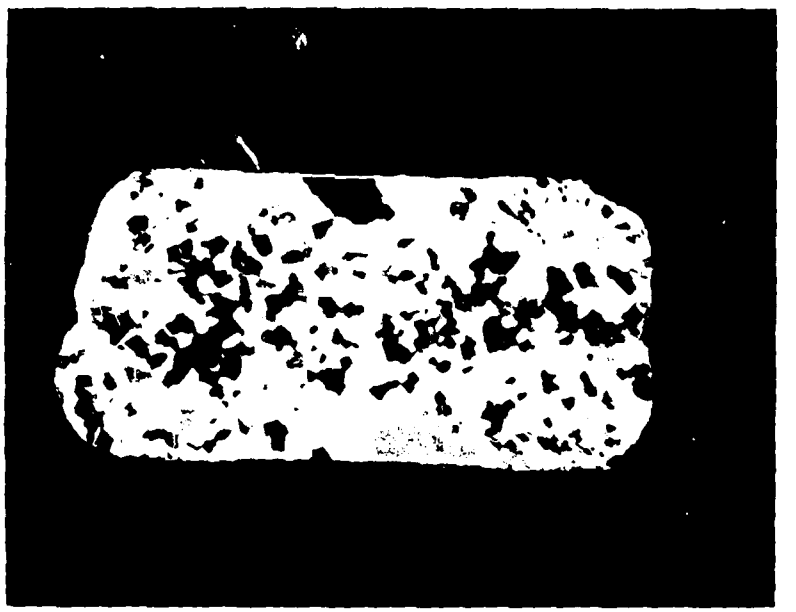

1000μm

4.0 REFERENCES

1. F. L. VerSnyder and R. W. Guard, Trans. ASM, 52, 485 (1960).

2. F. L. VerSnyder and M. E. Shank, Mat. Sci. Eng., 6, 213 (1970).

3. F. R. Thompson, F. D. George and E. M. Breinan, Proc. on the Conf. on In-Situ Composites, NMAB 308-2, 1972.

4. E. W. Kelley, Met. Eng. Q., 10, Feb. 1971.

5. A. R. Knott and C. H. Symonds, Metals Tech., 370, Aug. 1976.

6. J. B. Moore and R. L. Athey, Design News, 17, Jan. 1970.

7. A. F. Giamei and F. L. VerSnyder, Grain Boundaries in Engineering Materials, Claitor's, Baton Rouge, 1975.

8. J. C. Uy, Metals/Materials Today, March 1976.

9. A. F. Giamei, E. H. Kraft and F. D. Lemkey, New Trends in Materials Processing, ASM, 1976.

10. T. Z. Kattamis, J. Coughlin and M. C. Flemings, Trans. TMS-AIME, 239, 1504 (1967).

11. M. C. Flemings and R. Mehrabian, Solidification, ASM, 1971.

12. M. C. Flemings, Solidification Processing, McGraw Hill, New York, 1974.

13. A. F. Giamei and J. G. Tschinkel, Met. Trans. A, Sept. 1976.

14. C. P. Sullivan, A. F. Giamei and F. L. VerSnyder, Proc. 5th Int'l. Symp. on Special Melting, 525, Carnegie-Mellon, Pitt. Pa., 1975.

15. S. Fulop and H. F. McQueen, Superalloys - Processing, MCIC #72-10, 1972.

16. B. H. Kear, J. M. Oblak and W. A. Owczarski, J. Met., 24, 25 (1972).

17. J. W. Edington, Metals Technology, p 138, March 1976.

18. C. C. Law and A. F. Giamei, Met. Trans., 7A, 5 (1976).

19. C. C. Law, A. F. Giamei, and A. V. Karg, J. Mat. Sci., 29, 29 (1977).

20. R. A. Petcovic, M. J. Luton and J. J. Jones, Acta Met., 27, 1633 (1979).

21. G. Van Drunen and S. Saimoto, Met. Trans. A, 10A, 783 (1979).

5.0 PUBLICATIONS AND PRESENTATIONS FROM AFOSR SPONSORED WORK

A presentation on the orientation dependence of creep rates was made in the Fall Meeting of TMS-AIME, Milwaukee, WI in October 1979.

A presentation of the effects of Re on superalloy deformation was made at the Fall Meeting of TMS-AIME in Milwaukee, WI, October 1979.

A paper entitled "Rhenium Effect on Creep Behavior of Ni-base Superalloys" was presented at the annual EMSA meeting in Reno, Nevada, August 1980.

A paper entitled "Workability of High Strength Superalloys" will be presented at the International Symposium on Superplasticity and Forming in San Diego, CA, June 20-24, 1982.